PHYSICAL REVIEW D 84, 085007 (2011)

Phases of a two-dimensional large-N gauge theory on a torus

Gautam Mandal[1,*] and Takeshi Morita[2,†]

[1] Department of Theoretical Physics, Tata Institute of Fundamental Research, Mumbai 400 005, India
[2] Crete Center for Theoretical Physics Department of Physics University of Crete, 71003 Heraklion, Greece

(Received 22 July 2011; published 11 October 2011)

We consider two-dimensional large N gauge theory with D adjoint scalars on a torus, which is obtained from a $D+2$-dimensional pure Yang-Mills theory on T^{D+2} with D small radii. The two-dimensional model has various phases characterized by the holonomy of the gauge field around noncontractible cycles of the 2-torus. We determine the phase boundaries and derive the order of the phase transitions using a method developed in an earlier work (hep-th/0910.4526), which is nonperturbative in the 't Hooft coupling and uses a $1/D$ expansion. We embed our phase diagram in the more extensive phase structure of the $D+2$-dimensional Yang-Mills theory and match with the picture of a cascade of phase transitions found earlier in lattice calculations [4]. We also propose a dual gravity system based on a Scherk-Schwarz compactification of a D2 brane wrapped on a 3-torus and find a phase structure which is similar to the phase diagram found in the gauge theory calculation.

DOI: 10.1103/PhysRevD.84.085007 PACS numbers: 11.15.Pg, 11.10.Wx, 11.25.Tq

I. INTRODUCTION AND SUMMARY

Gauge theories on spaces with compact directions have been studied for a long time. As a prototypical example, $d+1$-dimensional Yang-Mills theory at a finite temperature T corresponds to a compactification of the (Euclidean) time direction on a circle of length $\beta = 1/T$. It is obviously important to study such a compactification to understand the physics of confinement/deconfinement transitions [1]. More generally, one can consider Yang-Mills theory on a compact space Σ. If the volume of Σ is finite, there is no sharp phase transition, but for an $SU(N)$ gauge theory in the large N limit, there are sharply demarcated phases depending on the shape and size parameters of Σ. In case the compact space is a torus, the phase diagram as a function of various radii (and coupling) reveals a rich phase structure [2,3], including a cascade of phase transitions in which the "Polyakov" loops along various noncontractible cycles become nonzero in succession as the radii are reduced [4,5]. Most of these studies are numerical (in the lattice or in the continuum) or, in some cases, based on holography (see Sec. VI for references and more details). One of the motivations of the present paper is to investigate these questions analytically in a simple situation, as explained below, by using and extending the "large-D" technique developed in [6].

To elaborate further, let us consider a Euclidean $d+D$-dimensional gauge theory[1] on a $d+D$-dimensional torus with radii L_μ[2]

$$S = \int_0^\beta dt \left(\prod_{M=1}^{D+d-1} \int_0^{L_M} dx^M \right) \frac{1}{4 g_{d+D}^2} \mathrm{Tr} F_{\mu\nu}^2. \qquad (1)$$

Here, the length of the temporal circle is denoted as $L_0 = \beta$ and the rest are denoted as L_M, $M = 1, \ldots, d+D-1$. The phases of (1) are characterized by Wilson lines around the $d+D$ noncontractible cycles of the torus:

$$W_\mu = \mathrm{Tr} U_\mu \equiv \frac{1}{N} \mathrm{Tr} P\left(\exp\left[i \int_0^{L_\mu} A_\mu dx^\mu \right] \right), \qquad (2)$$

where no sum over μ is intended. These Wilson loops transform nontrivially under the center symmetry.[3] For sufficiently large radii L_μ, all W_μ vanish, signifying unbroken center symmetry. In this phase, local gauge-invariant observables are independent of L_μ in the strict large N limit [9–11]. Since W_0 can be interpreted as $\exp[-S_q]$, where S_q is the action for a static quark, the phase with $\langle W_0 \rangle = 0$ exhibits confinement. As is well-known, as β is reduced (i.e. the temperature is increased), below a certain critical value β_c, $\langle W_0 \rangle$ becomes nonzero, signaling a deconfinement transition together with a breaking of the center symmetry $Z_N^{d+D} \to Z_N^{d+D-1}$. In this phase, the observables can depend on β but are still independent of L_i [10]. It has been argued from lattice studies (see [4]

*email: mandal@theory.tifr.res.in,
†takeshi@physics.uoc.gr

[1] In this paper, we will not consider the contribution of the θ term.

[2] Our notation for spacetime coordinates is $\{x^0 \equiv t, x^M\}$, $M = 1, \ldots, d+D-1$. We will further split the $d+D-1$ coordinates into d "large" dimensions $\{x_0, x^i\}$, $i = 1, \ldots, d-1$ and D "small" dimensions x^I, $I = 1, 2, \ldots D$ (the meaning of "large" and "small" is explained below).

[3] "Center symmetry"[7,8] is generated by quasiperiodic "gauge transformations" $\alpha(x^\mu) = \exp[2\pi i (n_\mu x^\mu / L_\mu) \mathcal{A}]$, where $\mathcal{A} = \mathrm{diag}[1/N, 1/N, \ldots, 1/N, (1-N)/N]$. The quasiperiodicity is up to phases $h_\mu = \exp[2\pi i n_\mu / N]$, $\mu = 0, 1, \ldots, d+D-1$ which parametrize $d+D$ copies of the center of $SU(N)$, Z_N^{d+D}. The $\alpha(x^\mu)$ are valid gauge transformations locally, and leave local color-singlets, e.g. $\mathrm{tr} F_{\mu\nu}^2$ invariant; in particular, they commute with the Hamiltonian. However, under the α-transformations, $W_\mu \to h_\mu W_\mu$. A nonzero value of $\langle W_\mu \rangle$ implies spontaneous symmetry breaking of the center symmetry in the μ-direction.

and Sec. VI for a review) that as the other radii are successively reduced, one has a cascade of analogous symmetry breaking transitions $Z_N^{d+D-1} \to Z_N^{d+D-2} \to \ldots \to 1$.

While it would be fascinating to study all the above phases analytically, in this paper we will be able to study the phases of a $D+2$-dimensional pure Yang-Mills theory on T^{D+2} (i.e. (1) with $d=2$) in which a D-dimensional torus (with radii $L^I/(2\pi)$, $I = 1, 2, \ldots, D$) is taken as small (ensuring broken Z_N symmetries in those directions), leaving the remaining $d=2$ directions (including time) of variable size. Such a theory is given by a Kaluza-Klein reduction[4] of (1) on the small T^D, and is described by the following action:

$$S = \int_0^\beta dt \int_0^L dx \,\mathrm{Tr}\bigg(\frac{1}{2g^2} F_{01}^2 + \sum_{I=1}^{D} \frac{1}{2}(D_\mu Y^I)^2 + \frac{m^2}{2}(Y^I)^2 - \sum_{I,J} \frac{g'^2}{4}[Y^I, Y^J][Y^I, Y^J]\bigg). \tag{3}$$

Here, Y^I comes from the gauge field components A_{I+1} and the covariant derivative is defined as $D_\mu = \partial_\mu - i[A_\mu, \,]$. A naive KK reduction leads to massless Y^I's and $g = g'$; however, a mass m for the adjoint scalars as well as radiative splitting between g and g' is induced from loops of KK modes (see Appendix A and Sec. II, respectively, for more details).

We should remark that (3) can either be regarded as a step towards understanding the full phase diagram of the $d+D$-dimensional theory (1), or be understood as a two-dimensional gauge theory in its own right. The spirit of the latter approach is to provide an example of an analytically solvable low-dimensional gauge theory in the limit of a large number of adjoint scalars (the $d=1$ theory was discussed in [6]). Equation (3), from this viewpoint, provides a bosonic counterpart of the Gross-Neveu model [13], where D plays the role of N_f, and the $SO(D)$-invariant bilinear $\sum_{I=1}^D Y_a^I Y_b^I$ of Sec. II A plays the role of $SU(N_f)$-invariant fermion bilinears such as $\sum_{i=1}^{N_f} \bar{\psi}_i \psi_i$ of the Gross-Neveu model.

Note that in this second point of view, where we regard the action (3) as an independent theory in its own right, the mass m can be taken to be arbitrary. In particular, if the mass is sufficiently large ($m^2 \gg g^2 ND$, $g'^2 ND$), the phase structure can be determined perturbatively [3,14]. However, as we will see in Appendix A, if we regard (3) as a KK reduction of (1) on T^D, then the mass m of the adjoint scalars is much lower than the scales mentioned above and the theory is not amenable to such perturbative methods. One of the goals of the present work is to provide a nonperturbative[5] analysis of (3) valid for any value of mass (including $m=0$), based on the "large-D" method developed in the previous work [6].

A few additional comments are in order:

(i) KK gauge theories have important applications to phenomenology [15–18]. Theories such as (3) provide important toy models in this context. In particular, issues such as different running of gauge couplings in the compactified and decompactified theories can be examined in such models. We will encounter some of these issues in Sec. II.

(ii) Gauge theories on compact spaces can sometimes have gravity duals. The deconfinement transition in $\mathcal{N}=4$ super Yang-Mills theory on $S^3 \times S^1$ [19,20] is a weak coupling continuation of the gravitational Hawking-Page transition [21,22]. Similar correspondences for two-dimensional supersymmetric gauge theories on tori were analyzed in [3,23].[6] In this paper, we will obtain (3) with $D=8$ from a Scherk-Schwarz compactification of a three-dimensional super Yang-Mills theory with 16 supercharges, which corresponds to the world volume theory of D2 branes. The latter theory has an AdS/CFT dual [24], which leads to the construction of a gravity dual for (3) in a sense defined in Sec. V.[7] As we will see, the gravity analysis will complement our knowledge of the phase structure from the gauge theory analysis.

(iii) Large N two-dimensional gauge theories themselves are interesting objects in the context of string theory and QCD. For instance, confinement/deconfinement type transitions [28] have been analytically found in 2D QCD with heavy adjoint scalars [14]. In addition, stringy excitations and glueball spectra have been obtained in 2D models in [29–33]. Thus, these models are good laboratories for real QCD. Our study, in fact, has a direct relevance for [32]; we hope to return to the issue of glueball spectrum discussed in this reference.

The principal result in this paper is the determination of some parts of the phase diagram of the two-dimensional theory (3) at weak coupling. The result is summarized in Fig. 4. The second result is the gravity analysis which

[4]The Kaluza-Klein reduction is tricky for gauge theories [3,11], since in the confined phase the KK modes can have energies $\sim 1/(NL)$, which become arbitrarily low at large N. The fractional modes, equivalent to the "long string" modes of [12], can be understood as arising from mode shifts of charged fields in the presence of Wilson lines whose eigenvalues are uniformly distributed along a circle (see Sec. II for an explicit verification for this statement). In the deconfined phase, however, the KK modes have energies $\sim 1/L$, like in ordinary field theories, and KK reduction proceeds as usual.

[5]in the 't Hooft coupling.

[6]For an extensive list of correspondences between low-dimensional gauge theories and gravitational systems, see [24–26].

[7]One of the motivations for this work was to construct a gauge theory dual to a dynamical Gregory-Laflamme transition. We will discuss this issue in a forthcoming publication [27].

complements the phase diagram at strong coupling, which is presented in Fig. 5.

The plan of the paper is as follows. In Sec.s II, III, and IV, we analyze the model (3) at weak coupling by using the $1/D$ expansion [34] developed in [6]. We find that the nature and the order of the confinement/deconfinement type transition depends on whether the size L of the spatial circle is large or small. For large L (which corresponds to the Tr$V = 0$ phase), we find (see Sec. II) a single first-order transition, thus providing analytical evidence for earlier lattice studies (see Sec. VI A for further details). On the other hand, for small L (corresponding to the Tr$V \neq 0$ phase), the analysis in [6] is valid and, as detailed in Sec. III, the transition consists of two higher order phase transitions. The phase diagram is summarized in Sec. IV in Fig. 4 and is in agreement with those from the lattice studies of [2,4,5]. We compare our results with these lattice studies and with [3] in Sec. VI.

To supplement our $1/D$ analysis of the gauge theory, we consider in Sec. V a dual gravity theory, obtained from D2 branes wrapped on a 3-torus with a Scherk-Schwarz circle. Although the gravity results pertain to thermodynamics in the strongly coupled regime, we observe that the phase structure is qualitatively similar to that of the weak coupling gauge theory. This allows us to arrive at a conjectured phase diagram in Fig. 5, which suggests a particular way of connecting the phase boundaries of Fig. 4.

In Sec. VI C, we comment on the dependence of the order of phase transition on the topology of the compact space. In Appendix A, we discuss the masses of the adjoint scalars which appear from integration of the KK modes at the one-loop level. In Appendix B, we fill in some details needed in Sec. II for integrating out the adjoint scalars. In Appendix C, we discuss the influence of the mass term in (3) on the phase diagram. In Appendix D, we provide important details of our gravity analysis.

II. CONFINEMENT/DECONFINEMENT TYPE TRANSITION IN LARGE RADIUS TORUS

In this section, we will analyze the confinement/deconfinement type transition in (3) for large L. First, (in Sec. II A) we will integrate out the adjoint scalars Y^I in a $1/D$ expansion, in a manner similar to [6], leading to the effective Hamiltonian (23) in the large L limit. Next, (in Sec. II B) we use, at $L \to \infty$, the results of [14,35,36], who studied this effective action in slightly different contexts, to determine the phase structure of our theory (3) at large L. The justification for extrapolating their result to finite L, as detailed below, comes from the phenomenon of large N volume independence [9–11] which is valid as long as L is large enough to ensure Tr$V = 0$.

To keep the analysis simple, in this section we consider (3) with $m = 0$, and defer the case of nonzero mass to Appendix C. As we will find there, the inclusion of the mass term does not change the qualitative structure of the different phases.

A. Large-D saddle point

In this section, we will generalize the analysis of the $0 + 1$-dimensional gauge theory [6] to the $d = 2$ model (3) and show that if we consider the number D of adjoint scalars to be large, the theory can be considered to be in the vicinity of a large-D saddle point[8] and various quantities such as the free energy and the mass gap etc. can be computed around the saddle point in a $1/D$ expansion.

As mentioned above, in this section we will consider (3) with $m = 0$. Introducing an auxiliary field B_{ab}, the path-integral of the gauge theory can be rewritten as

$$Z = \mathcal{N} \int \mathcal{D}B\mathcal{D}A_\mu \mathcal{D}Y^I e^{-S(B,A,Y)},$$

$$S(B, A, Y) = \int_0^\beta dt \int_0^L dx \bigg[\frac{1}{2g^2} F_{01}^{a2} + \frac{1}{2}(D_\mu Y_a^I)^2 - i\frac{1}{2} B_{ab} Y_a^I Y_b^I + \frac{1}{4g'^2} B_{ab} M^{-1}_{ab,cd} B_{cd} \bigg], \tag{4}$$

where $\mathcal{N}$ is a constant factor and we have used the following matrix,

$$M_{ab,cd} = -\frac{1}{4}\{\mathrm{Tr}[\lambda_a, \lambda_c][\lambda_b, \lambda_d] + (a \leftrightarrow b) + (c \leftrightarrow d) + (a \leftrightarrow b, c \leftrightarrow d)\}, \tag{5}$$

λ^a ($a = 1, \cdots, N^2 - 1$) being the generators of $SU(N)$. Our approach, similar to the one-dimensional case, will be as follows. We will integrate out the Y^I's to obtain an effective action for A_μ and B_{ab}, and find a saddle-point solution for B_{ab} (for given A_μ) in a large-D limit. The effective action for A_μ will be essentially obtained by substituting the saddle-point value of B_{ab} in this effective action.

As in [6], it is convenient to decompose B_{ab} as the sum of a trace piece (independent of x, t) and an orthogonal part:

$$B_{ab}(t) = i\Delta^2 \delta_{ab} + g' b_{ab}(t, x), \tag{6}$$

where b_{ab} satisfies $\int dt \int dx b_{aa} = 0$. Such a decomposition, into a large diagonal piece and a small off-diagonal fluctuation, will be *a posteriori* justified by finding a saddle point for B_{ab} of the form $\langle B_{ab} \rangle = i\Delta_0^2 \delta_{ab}$, where Δ_0 is a real constant (depending only on the 't Hooft coupling).

[8] Although the saddle point arises in a manner similar to that in four-fermion models such as Gross-Neveu or Nambu Jona-Lasinio, the saddle point is *complex*. See [6] for details.

With this decomposition, the action reduces to

$$
\begin{aligned}
S_0 &= -\frac{\beta L N \Delta^4}{8 g'^2}, \\
S_1 &= \int_0^\beta dt \int_0^L dx \bigg(\frac{1}{2g^2} F_{01}^{a2} + \tfrac{1}{4} b_{ab} M^{-1}_{ab,cd} b_{cd} \\
&\qquad + \tfrac{1}{2} (D_\mu Y_a^I)^2 + \tfrac{1}{2} \Delta^2 Y_a^{I2} \bigg), \\
S_{\rm int} &= -\int_0^\beta dt \int_0^L dx \bigg(\frac{ig'}{2} b_{ab} Y_a^I Y_b^I \bigg),
\end{aligned} \tag{7}
$$

where we have used $M^{-1}_{ab,cd}\delta_{cd} = \delta_{ab}/2N$ [6]. Let us now take a large-D limit,

$$
\begin{aligned}
&g, g' \to 0, \qquad N, D \to \infty \qquad s.t. \\
&\tilde{\lambda} \equiv g^2 DN, \qquad \tilde{\lambda}' \equiv g'^2 DN \qquad \text{fixed.}
\end{aligned} \tag{8}
$$

To the leading order of this expansion, we can ignore the interaction term $S_{\rm int}$.[9] In that case, the integration of b_{ab} will contribute just a numerical factor and we will ignore it. Integrating over the Y^I's in S_1, we then get the following leading result for the partition function

$$
\begin{aligned}
Z &= \int \mathcal{D}A \mathcal{D}\Delta e^{-S_{\rm eff}[A,\Delta]}, \\
S_{\rm eff}[A,\Delta] &= -\frac{\beta L N \Delta^4}{8g'^2} + \int_0^\beta dt \int_0^L dx \frac{1}{2g^2} F_{01}^{a2} + \delta S_{\rm eff},
\end{aligned} \tag{9}
$$

where $\delta S_{\rm eff}$ is the 1-loop contribution from the Y^I-integration:

$$
\delta S_{\rm eff}[A,\Delta] = \frac{D}{2} \,\mathrm{logdet}(-D_\mu^2 + \Delta^2). \tag{10}
$$

It is difficult to evaluate this last quantity in general. However, using arguments similar to [3], we will find that:

(a) If $\Delta^2 \gg \tilde{\lambda} \equiv g^2 DN$ (this assumption will be justified in (19)), terms in $\delta S_{\rm eff}$ involving derivatives of A_μ, e.g. terms involving the gauge field strength and its covariant derivatives are suppressed.

(b) If $L\Delta \gg 1$,[10] we can approximately treat A_0 and A_1 as commuting matrices.

The argument for assertion (a) can be sketched briefly as follows. Consider the simplest of the 1-loop diagrams (Fig. 1) which contribute to (10) and has only two external gauge field insertions: For large Δ, the Y^I-propagator in the loop carrying momentum p can be expanded in powers of p^2/Δ^2. The first term in that expansion goes as $ND(k_\mu k_\nu - k^2 g_{\mu\nu})/\Delta^2$ (in the Feynman gauge), where the factors of N and D come from the Y^I-loop, and k is the external momentum going into the loop. This term amounts to a correction, to the F_{01}^2/g^2 term, of the form $[1 + O(\tilde{\lambda}/\Delta^2)]$, as claimed above. We will ensure below that $\tilde{\lambda}/\Delta^2 \ll 1$.

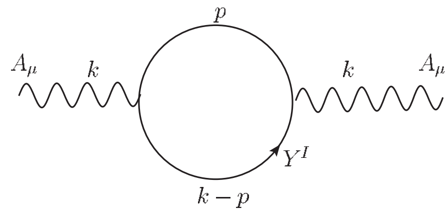

FIG. 1. A simple Feynman diagram contributing to (10).

The argument for assertion (b) will follow *a posteriori* after we proceed with the assumption that A_μ are constant commuting matrices. Under this assumption, as detailed in Appendix B, the one-loop term becomes

$$
\begin{aligned}
\delta S_{\rm eff} = \frac{D\beta L}{8\pi^2} \bigg[& N^2 (-\pi\Lambda^2 + \pi(\Lambda^2 + \Delta^2)\log(\Lambda^2 + \Delta^2) \\
& - \pi \Delta^2 \log \Delta^2) - \sum_{(k,l)\neq(0,0)} |\mathrm{Tr}(U^k V^l)|^2 \\
& \times \frac{4\pi\Delta}{\sqrt{(\beta k)^2 + (Ll)^2}} K_1\Big(\Delta\sqrt{(\beta k)^2 + (Ll)^2}\Big)\bigg].
\end{aligned} \tag{11}
$$

Here, we have used a momentum cutoff Λ to regulate the determinant,[11] and used the notations $U = e^{i\beta A_0}$ and $V = e^{iLA_1}$. K_1 is the modified Bessel function of the second kind. Using the asymptotic expansion $K_1(z) = \sqrt{\pi/2z}e^{-z} + \cdots$ for large z (justified below) and omitting some irrelevant divergent terms, we get

$$
\begin{aligned}
\delta S_{\rm eff} = \frac{DN^2\beta L}{8\pi} \bigg[& (\Lambda^2 + \Delta^2) \log\Big(1 + \frac{\Lambda^2}{\Delta^2}\Big) \\
& + \Delta^2 \log\Big(\frac{\Lambda^2}{\Delta^2}\Big)\bigg] - \frac{D}{\sqrt{2\pi}} \bigg(L\sqrt{\frac{\Delta}{\beta}} e^{-\Delta\beta} |\mathrm{Tr}U|^2 \\
& + \beta \sqrt{\frac{\Delta}{L}} e^{-\Delta L} |\mathrm{Tr}V|^2 \bigg) + \cdots,
\end{aligned} \tag{12}
$$

where the $\cdots$ terms represent higher order terms in $e^{-\Delta\beta}$, $e^{-\Delta L}$. Since we are interested in large L, it is obvious why higher order terms in $e^{-\Delta L}$ should be ignored. We now have an *a posteriori* justification for having ignored terms involving commutators $[U, V]$; the smallest gauge-invariant such term would have at least

[9] In the one-dimensional model ($d = 1$), the next order of the $1/D$ expansion has been evaluated in [6]. There, such $1/D$ corrections do not change the nature of the phase structure. We can expect that the same thing will happen in our two-dimensional gauge theory also. Hence, we do not evaluate the $1/D$ corrections in this article.

[10] This assumption will be justified later in what we will define as the "large L regime" $L \gtrsim L_c$ (see (33) and (32)), since $L_c\Delta$ will turn out be large, using (19).

[11] The cutoff Λ should be smaller than M_{KK}, which is the inverse length scale of the D-dimensional compactification torus.

two Us and two Vs and hence are expected to be of the same order as the U^2V^2 term in (11), and hence can be ignored [3]. Higher order terms in $e^{-\Delta\beta}$ are ignored because they will be small in the region of parameter space in which interesting phase structures will appear. We will ensure this at the end of Sec. II B [see comment (a) below (32)].

In the $L \to \infty$ limit, we can ignore the term in (12) involving V. Let us integrate Δ from (9) under this assumption and derive the effective action for the U-variable. The saddle-point equation with respect to Δ^2 reads as

$$-\frac{\beta L\Delta^2}{2\tilde{\lambda}'} + \frac{\beta L}{4\pi}\log\left(1+\frac{\Lambda^2}{\Delta^2}\right) + \frac{L}{\sqrt{2\pi}}\sqrt{\frac{\beta}{\Delta}}e^{-\Delta\beta}\left(1-\frac{1}{2\Delta\beta}\right)\left|\frac{1}{N}\,\mathrm{Tr}U\right|^2 + \cdots = 0. \tag{13}$$

In the $\mathrm{Tr}U = 0$ phase (which is realized for sufficiently large β), $\Delta = \Delta_0$ is determined implicitly from the equation

$$\tilde{\lambda}' = \frac{2\pi\Delta_0^2}{\log(1+\frac{\Lambda^2}{\Delta_0^2})}. \tag{14}$$

This equation can be viewed as a renormalization condition which assigns a Λ-dependence to $\tilde{\lambda}'$ such that the physical mass scale Δ_0 is held fixed. Here, Δ_0 plays a role analogous to Λ_{QCD} and its choice specifies the theory. We will, in fact, choose it in such a way as to ensure the condition[12]

$$\tilde{\lambda} \sim \tilde{\lambda}' \quad \text{at } \Lambda = M_{KK}. \tag{15}$$

As β decreases, $\mathrm{Tr}U$ eventually becomes nonzero. However, near criticality, $\beta\Delta \gg 1$ (this is justified because of (19) and (32)). Therefore, we can solve (13) for Δ in the form $\Delta_0 + O(\exp[-\beta\Delta_0])$. We will write the explicit solution only for $\Lambda \gg \Delta$:

$$\Delta = \Delta_0 + \frac{1}{2\pi\Delta_0^2/\tilde{\lambda}' + 1}\sqrt{\frac{2\pi\Delta_0}{\beta}}e^{-\Delta_0\beta}\left|\frac{1}{N}\,\mathrm{Tr}U\right|^2 + \cdots, \tag{16}$$

where

$$\Delta_0 = \sqrt{\frac{\tilde{\lambda}'}{2\pi}W\left(\frac{2\pi\Lambda^2}{\tilde{\lambda}'}\right)}, \tag{17}$$

and $W(z)$ is the Lambert's W function defined implicitly by the equation $z = W(z)e^{W(z)}$. Note that, by using an expansion $W(z) = \log z - \log(\log z) + \cdots$ for large z, we obtain

$$\Delta_0 = \sqrt{\frac{\tilde{\lambda}'}{2\pi}\log\left(\frac{2\pi\Lambda^2}{\tilde{\lambda}'}\right)} + \cdots. \tag{18}$$

Imposing the renormalization condition (15), we then obtain a relation[13]

$$\Delta_0^2/\tilde{\lambda} \sim \frac{1}{2\pi}\log\left(\frac{2\pi M_{KK}^2}{\tilde{\lambda}}\right) \gg 1. \tag{19}$$

Thus, we confirmed that the assertion (a) above is satisfied. Substituting (16) in S_{eff} in (9) and ignoring the term involving $\mathrm{Tr}V$, we get the following effective action for A_μ:

$$\frac{S(A)}{DN^2} = C(\tilde{\lambda}', \Delta_0) + \int_0^\beta dt\int_0^L dx\left(\frac{1}{2\tilde{\lambda}N}F_{01}^{a2} - \frac{1}{\sqrt{2\pi}}\sqrt{\frac{\Delta_0}{\beta^3}}e^{-\Delta_0\beta}\left|\frac{1}{N}\,\mathrm{Tr}U\right|^2\right) + \cdots, \tag{20}$$

$$C(\tilde{\lambda}', \Delta_0) = \frac{\beta L\Delta_0^2}{8\pi}\left(1+\frac{\pi\Delta_0^2}{\tilde{\lambda}'}\right), \tag{21}$$

where the terms $\cdots$ are higher order in the same sense as in (12). We have used $\int dxdt|\mathrm{Tr}U|^2 = L\beta|\mathrm{Tr}U|^2$ which is correct up to derivatives of U which occur at $O(\tilde{\lambda}/\Delta^2)$ and are small, as argued above.

In the limit of $L \to \infty$,[14] we can choose the gauge $A_1 = 0$. Solving the Gauss's law condition in this gauge, we get $A_0 = (g^2/\partial_x^2)\varrho$, where $\varrho \equiv -\frac{i}{2}[Y^I, \partial_t Y^I]$ is the charge density; in the large-D saddle point, especially for large enough Δ_0, the condensate is static and temporal fluctuations of ϱ, and consequently, of A_0, are suppressed. As a result, we can write

$$\int dxdt\,\mathrm{Tr}F_{01}^2 = \beta\int dx\,\mathrm{Tr}(\partial_x A_0)^2 = \beta^{-1}\int dx\,\mathrm{Tr}|\partial_x U|^2,$$

where

[12]This follows from the fact that the distinction between g and g' in (3) vanishes in the original pure YM theory (1). In order to fix the precise coefficient of the renormalization condition (15), we need to evaluate the contribution of the mass (C3) and the running of g and g' for scales larger than M_{KK}. The value of mass and the running of the couplings depend on the details of the higher-dimensional theory. If we are interested in the two-dimensional gauge theory (3) itself as in the comment (iii) in the introduction, the renormalization condition that replaces (15) is arbitrary. However, even in that case, the qualitative nature of the phase structures in this paper does not change as long as $(\Delta_0^2 + m^2)/\tilde{\lambda} \gg 1$ is satisfied.

[13]The inequality follows from the condition $\tilde{\lambda}/M_{KK}^2 \ll 1$, which is necessary for a KK reduction. This condition implies that the dimensionless 't Hooft coupling is small: $\tilde{\lambda}_{D+2}M_{KK}^{D-2} \ll 1$.

[14]Although we are apparently taking $L \to \infty$ here, as we discuss at the end of the next subsection, we can extend these results to finite L which is large enough to ensure vanishing ot $\mathrm{Tr}V$. Note that if $\mathrm{Tr}V \neq 0$, the $1/D$ expansion does not work at $L \to \infty$ as argued in [37], where such a situation is discussed in the presence of R-symmetry chemical potential.

$$U(x) = P\exp\left[i\int_0^\beta dt A_0(x,t)\right] = \exp[i\beta A_0(x)]. \quad (22)$$

By rescaling $x \to x' = \tilde{\lambda}\beta x$, we eventually get an effective action in terms of $U(x)$

$$S/DN^2 = C(\tilde{\lambda}', \Delta_0) + \int_{-\infty}^{\infty} dx\left[\frac{1}{2N}\mathrm{Tr}(|\partial_x U|^2) - \frac{\xi}{N^2}|\mathrm{Tr}U|^2\right], \quad (23)$$

where

$$\xi = \sqrt{\frac{\Delta_0}{2\pi\tilde{\lambda}^2\beta^3}}e^{-\Delta_0\beta}. \quad (24)$$

Note that ξ is a monotonically decreasing function of β.

Equations similar to (23) and (24) have earlier been derived in [14] who consider a two-dimensional gauge theory with heavy adjoint scalars of mass m. In their equations, m appears in place of Δ_0. We could have, in fact, derived the above effective action (23) as follows: the large-D saddle point generates a dynamical mass Δ_0 for the adjoint scalars which turns the theory into a massive adjoint scalar QCD; once this is established, we can use the method of [14] with $m = \Delta_0$, to arrive at (23). The agreement with the results of [14] provides an additional check on our derivation. Adjoint scalar QCD with large scalar mass has also been considered by [3] who have independently derived equations analogous to (23) and (24); our method of derivation follows their derivation closely, except that our mass is dynamically generated, as mentioned above. The discussion in Appendix C involving arbitrary m relates the two extreme cases of large mass and zero mass.

B. The phase transition at large L

Phase transitions in the system (23) have been discussed in [14,35,36]. We will adopt their result to infer about phase transitions in our two-dimensional gauge theory (3) at large L [the range of L is defined in (33)]. For completeness, we will briefly review some of the results in these papers.

If we regard the coordinate x in (23) as time, it becomes the quantum mechanics of a single unitary matrix, a subject that has been extensively studied [38–44]. Phases of such a model can be described by the behavior of the eigenvalue density

$$\rho(\theta, x) = \frac{1}{N}\sum_{i=1}^{N}\delta[\theta - \theta_i(x)], \quad (25)$$

where $\exp[i\theta_i(x)]$ are the eigenvalues of (22).

The Hamiltonian of this system (regarding x as time) can be written as [39–44]

$$H = \int d\theta\left(\frac{1}{2}\rho v^2 + \frac{\pi^2}{6}\rho^3\right) - \xi|u_1|^2 - \frac{1}{24}, \quad (26)$$

where we have ignored the constant term C in (23). Here, $v = \partial_\theta\Pi$, and $\Pi(\theta, x)$ is the canonical conjugate of $\rho(\theta, x)$. We have also used the notation $u_n = \frac{1}{N}\mathrm{Tr}U^n$, $u_{-n} = (u_n)^*$. Note that $u_n(x)$ are moments of the eigenvalue density (25):

$$\rho(\theta, x) = \frac{1}{2\pi}\sum_{n=-\infty}^{\infty}u_n(x)e^{-in\theta}. \quad (27)$$

To study the various equilibrium phases of the system, we study static solutions of (26), which [14,35,36] are given by $v(\theta) = 0$ and

$$\rho(\theta) = \frac{\sqrt{2}}{\pi}(\sqrt{E + 2\xi\rho_1\cos\theta}), \quad (28)$$

where $\rho_1 = u_1 = u_1^*$ is the first moment (real in this case), which must self-consistently satisfy [see (27)]

$$\int_0^{2\pi} d\theta\rho(\theta)\cos\theta = \rho_1. \quad (29)$$

The constant E is fixed by solving the normalization condition

$$\int_0^{2\pi} d\theta\rho(\theta) = 1. \quad (30)$$

Depending on the value of the constant ξ in (26), Eq. (30) may not determine E uniquely. In general, we obtain three branches $E(\xi)$, depending on whether (28) describes a uniform, nonuniform, or gapped eigenvalue distribution (see Fig. 2). The value of $E(\xi)$ in these three cases is different. The thermodynamic stability for the various branches of the function $E(\xi)$ is analyzed [14,35,36] by comparing the values of the Euclidean Hamiltonian (26) which can also be regarded as the free energy. They can be summarized as follows:

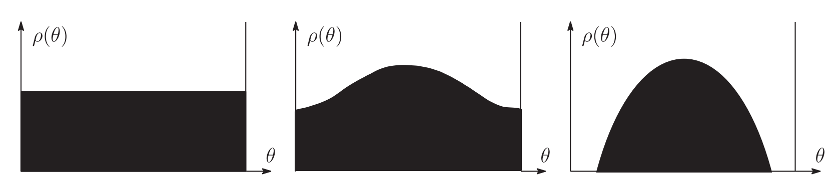

FIG. 2. Configurations of eigenvalue density $\rho(\theta)$ in the unitary matrix model. The left plot is the uniform distribution [corresponding to $\rho_1 = 0$ in (28)], the middle one is the nonuniform distribution ($|E/(2\xi\rho_1)| \geq 1$), and the right one is the gapped distribution ($|E/(2\xi\rho_1)| \leq 1$).

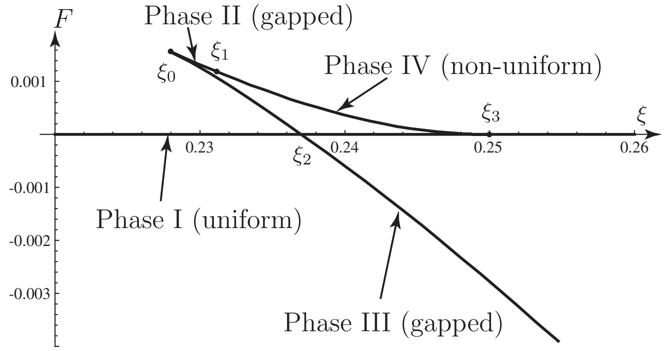

FIG. 3. Free energy (26) vs ξ in the four phases. The gapped and nonuniform solutions here are numerically evaluated. Since ξ is a monotonically increasing function of temperature [see (24)], the uniform distribution (Phase I) is stable at low temperatures and the gapped distribution (Phase III) is stable at higher temperature. A first-order phase transition between these two phases happens at ξ_2.

(i) Independent of the value of ξ, the uniform solution always exists. We call this phase as I.
(ii) For $\xi < \xi_0 = 0.227$, only one solution (phase I) exists and is stable.
(iii) At $\xi = \xi_0$, there is nucleation of two gapped solutions. One is unstable (phase II) and another is meta-stable (phase III).
(iv) At $\xi = \xi_1 = 0.23125$, a GWW type phase transition [38,45] occurs in phase II and the gapped solution becomes a solution with nonuniform distribution (Phase IV).
(v) At $\xi = \xi_2 = 0.237$, there is a first order phase transition between the phases I and III. Above ξ_2, the phase III is stable and the phase I is metastable.
(vi) At $\xi = \xi_3 = 1/4$, phase IV merges into phase I, and the uniform solution becomes unstable beyond ξ_3.

These are summarized in Fig. 3.

Using (24), we can read off the critical temperatures corresponding to these transition points:

$$\beta_m \equiv \beta(\xi_m) = \frac{3}{2\Delta_0} W\left[\frac{2}{3(2\pi\xi_m^2)^{1/3}}\left(\frac{\Delta_0^2}{\tilde{\lambda}}\right)^{2/3}\right]$$
$$\approx \frac{1}{\Delta_0}\left(\log\left(\frac{\Delta_0^2}{\tilde{\lambda}}\right) - 1.53 - \log\xi_m\right),$$
$$m = 0, 1, 2, 3. \tag{31}$$

Here, Lambert's W function is employed again. In the second step, we have assumed $\Delta_0^2/\tilde{\lambda} \gg 1$ and $\xi_m = O(1)$.

As we come down from $\beta = \infty$ (go up in temperature), there is a first-order phase transition at β_2 from the center symmetric phase ($\mathrm{Tr}U = 0$) to the broken symmetry phase ($\mathrm{Tr}U \neq 0$) at an inverse temperature

$$\beta_{\mathrm{cr}} \equiv \beta_2 \approx \frac{1}{\Delta_0}\log\left(\frac{\Delta_0^2}{\tilde{\lambda}}\right). \tag{32}$$

Several comments are in order here:

(a) The assumption, used in Sec. II A, that $e^{-\Delta\beta}$ is small, is correct in the parameter region we are interested in. The interesting phase structures appear in the regime $\xi \sim O(1)$. Thus, since $\tilde{\lambda}/\Delta_0^2 \ll 1$ [see (19)], $e^{-\Delta\beta} \sim e^{-\Delta_0\beta} \ll 1$ from (31). Therefore, the terms in (11) involving U^n, $n = 2, 3, \ldots$ are suppressed.
(b) The Euclidean model (3) is symmetric under the interchange of $(t, \beta) \leftrightarrow (x, L)$. Hence, similarly to (32), we can deduce a phase transition in L from the $\mathrm{Tr}V = 0$ phase to $\mathrm{Tr}V \neq 0$ (at large enough β) at a critical length $L_{\mathrm{cr}} = \beta_{\mathrm{cr}}$.
(c) The existence of a finite L_{cr} above confirms that the transition which we found at $L \to \infty$ and $\beta = \beta_{\mathrm{cr}}$ between $\mathrm{Tr}U = 0$ and $\mathrm{Tr}U \neq 0$ indeed happens in the $\mathrm{Tr}V = 0$ phase. Therefore, the expression for β_{cr} is valid even at finite L as long as $\mathrm{Tr}V = 0$, since large N volume independence [9,10] ensures that gauge-invariant quantities like the free energy and the vacuum expectation value (vev) of Wilson loop operators do not depend on L in the $\mathrm{Tr}V = 0$ phase. Thus, the correct definition of "large L" in this section is

$$L \gg L_{\mathrm{cr}} = \beta_{\mathrm{cr}}, \tag{33}$$

which ensures that we are in the $\mathrm{Tr}V = 0$ phase. β_{cr} is defined in (32).
(d) By considering the interchange $\beta \leftrightarrow L$, we can claim that, if there is no direct transition from $\mathrm{Tr}U = \mathrm{Tr}V = 0$ phase to $\mathrm{Tr}U \neq 0$ $\mathrm{Tr}V \neq 0$ phase, the two transition line $\beta = \beta_{\mathrm{cr}}$ and $L = L_{\mathrm{cr}}$ meet at $\beta = L = \beta_{\mathrm{cr}}$. See Fig. 4.[15]
(e) As we discuss in Appendix C, the nonzero mass in (3) does not change the qualitative nature of the phase structure.

III. PHASE TRANSITIONS AT SMALL L

In this section, we discuss the phase structure for small L ($L \ll L_{\mathrm{cr}}$). In this case, we can dimensionally reduce the theory (see footnote 4) to obtain the action (B1) with $d = 1$. Hence, we can use the analysis in [6][16] where the phase structure has been studied by using the $1/D$ expansion. The phases are characterized by the eigenvalue density (27). Here, we summarize the results of [6],

[15]Note that a transition line between $\mathrm{Tr}U = \mathrm{Tr}V = 0$ phase and $\mathrm{Tr}U \neq 0$ $\mathrm{Tr}V \neq 0$ phase, if it exists (e.g. as in the third circled option in Fig. 4), could depend on L and β. However, the gravity analysis in Sec. V suggests that there is no such transition in our model, consistent with the "cascade picture" reviewed in Sec. VI. In this case, as represented by the second joining option in Fig. 4, (33) can be relaxed to $L > L_{\mathrm{cr}}$.

[16]In [6], we had considered massless adjoint scalars. We generalize the results to nonzero mass in Appendix C.

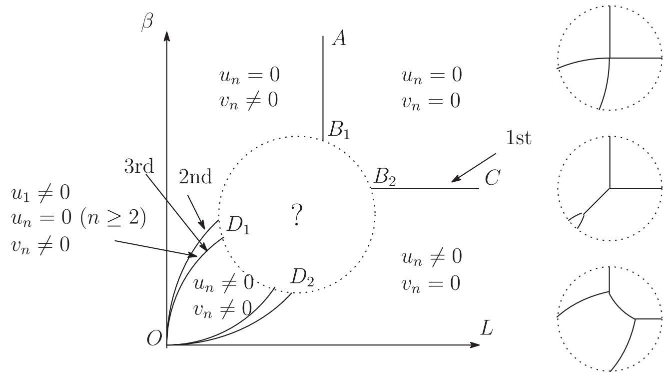

FIG. 4. Phase structure of the 2d gauge theory at weak coupling (defined below). There are essentially four phases characterized by nonzero values of various Wilson lines. The inner region, with both Wilson lines nonzero, includes two additional phases in which the eigenvalue distribution is gapless but nonuniform. The orders of the phase transitions (1st, 2nd, 3rd) are indicated. Our analysis does not apply to the region enclosed by the dotted lines. Possible connections between the phase boundaries across this region are suggested in the inset (where boundaries of the intermediate phases are omitted for simplicity). A similar diagram is proposed in [3] for the model (3) with large mass for the adjoint scalars (see Sec. VI B for details). As we will see in Fig. 5, the gravity analysis conforms to the second pattern. We will see in Sec. VI A that the second pattern is also supported by lattice studies.

(i) $\beta > \beta_{c1}$: The stable solution is given by $u_n = 0$ $(n \geq 1)$. The eigenvalues of A_0 are distributed uniformly.
(ii) $\beta_{c1} > \beta > \beta_{c2}$: The stable solution is given by $u_1 \neq 0$, $u_n = 0$ $(n \geq 2)$. The eigenvalue distribution is nonuniform and gapless.
(iii) $\beta_{c2} > \beta$: The stable solution is given by $u_n \neq 0$ $(n \geq 1)$. The eigenvalue distribution is gapped.
(iv) The phase transition at $\beta = \beta_{c1}$ is of second order and the transition at $\beta = \beta_{c2}$ is a third order (GWW type) transition.

The critical temperatures are calculated up to $O(1/D)$ in [6][17] as

$$\beta_{c1}\tilde{\lambda}_1^{1/3} = \log\tilde{D}\left[1 + \frac{1}{\tilde{D}}\left(\frac{203}{160} - \frac{\sqrt{5}}{3}\right)\right], \tag{34}$$

$$\beta_{c2}\tilde{\lambda}_1^{1/3} - \beta_{c1}\tilde{\lambda}_1^{1/3} = \frac{\log\tilde{D}}{\tilde{D}}\left\{-\frac{1}{6} + \frac{1}{\tilde{D}}\left[\left(-\frac{499073}{460800} + \frac{203\sqrt{5}}{480}\right)\log\tilde{D} - \frac{1127\sqrt{5}}{1800} + \frac{85051}{76800}\right]\right\}, \tag{35}$$

[17]Eqs. (34) and (35) are calculated for $m = 0$. The massive case is discussed in Appendix C. Note that the mass from the KK modes for $d = 1$ is proportional to $\sqrt{\lambda_1 L}$ as in (A6). Thus, the mass correction is small for small L.

where $\tilde{D} = D + 1$ and $\tilde{\lambda}_1 = (g')^2 N(D+1)/L$. In the β-L plane, the transition lines appear as curves $\beta \propto L^{1/3}$ passing through the origin. Since our analysis is valid only for $L \ll L_{\rm cr}$, we should trust these transition lines only in that region, as we have depicted in Fig. 4. By using the $\beta \leftrightarrow L$ reflection symmetry, we can also infer phase transition lines for $\beta \ll \beta_{\rm cr}$ described by $L \propto \beta^{1/3}$, as shown in Fig. 4.

Contrary to the case of large L, an intermediate nonuniform phase exists at small L. A similar feature in the context of higher order confinement/deconfinement type phase transitions has been seen in [20].

We should mention that considerations in this section are valid up to $\tilde{\lambda}' \lesssim \lambda_{\max}$ where $\lambda_{\max} = L/\beta^3$ for $\beta \ll \beta_{\rm cr}$, and $\lambda_{\max} = \beta/L^3$ for $L \ll L_{\rm cr}$ [6], which can be large close to the origin (See footnote 34 also.). We will come back to this point in Sec. V.

IV. PHASES OF 2D GAUGE THEORY ON T^2

In the last two sections, we have studied confinement/deconfinement type transitions in the model (3) for large and small values of the spatial size L.

We have found that the nature of the transition depends on L. We can summarize these results in Fig. 4, where we supplemented our calculations with the reflection symmetry $\beta \leftrightarrow L$ of the model.

Weak coupling in the above diagram (Fig. 4), for large L (or large β), is defined by $\tilde{\lambda}/\Delta^2 \ll 1$ [see assumption (a) below (10)]. In case the 2d gauge theory is obtained from a KK reduction, the above notion of weak coupling translates to $\tilde{\lambda} \ll M_{KK}^2$ (see (19) and footnote 12). For small L (or β), the coupling should satisfy $\tilde{\lambda}' \lesssim \beta/L^3$ (or L/β^3) to validate the additional KK reduction to one dimension; as remarked at the end of Sec. III, this limit on $\tilde{\lambda}'$ can be quite large close to the origin of Fig. 4.

As mentioned in the Introduction, our model (3) can be regarded as a dimensional reduction of a $D+2$-dimensional pure Yang-Mills theory compactified on a small T^D. For the dimensional reduction to work (see footnote 4), $W_I = {\rm Tr}U_I$ $(I = d, \cdots, d+D-1)$ must be nonzero (which is ensured by a sufficiently small size of the D-dimensional torus). Therefore, we can regard the phase structure in Fig. 4 as a part of the $D+2$-dimensional pure Yang-Mills theory in the $W_I \neq 0$ phase. Such a Yang-Mills theory on T^3 and T^4 have been studied in lattice gauge theory and we will compare our results with those studies in Sec. VI.

Since our phase structure is derived through the $1/D$ expansion, it is not *a priori* obvious whether the result should be valid for small D. However, at least for small L, the comparison with numerical studies [46–48], as explained in [6], turns out to be remarkably good even for small D. For example, for $D = 2$ the $1/D$ expansion, performed up to an accuracy of $O(1/D)^2$ reproduces numerical results within the expected 25%. Thus, we believe that the phase structure in the large L region also should be qualitatively correct for small D ($D \geq 2$).

V. THE PHASE STRUCTURE FROM GRAVITY

In the previous sections, we evaluated the phase structure of the bosonic gauge theory (3) at weak coupling. In this analysis, it was difficult to figure out the phase structure of the middle region, namely, where both β and L have intermediate values. In particular, it was not clear how the various phase boundaries in Fig. 4 are connected.

In this section, we attempt to construct a gravitational dual of our system along the lines of Witten's realization of the 4d pure Yang-Mills theory [22]. We consider IIA supergravity on $R^7 \times T^3$ ($T^3 = S^1_\beta \times S^1_L \times S^1_{L_2}$) and put N D2 branes on the T^3. The AdS/CFT duality in this context is discussed in [24] and more details are provided in Appendix D. The dual gauge theory is three-dimensional $\mathcal{N} = 8$ $SU(N)$ super Yang-Mills on T^3, with the identifications $(t, x_1, x_2) = (t + \beta, x_1 + L, x_2 + L_2)$. In order to complete the definition of the theory, we need to choose a boundary condition of the fermions along each compact direction. Let us impose an antiperiodic boundary condition on the fermions on the x_2 cycle. If L_2 is sufficiently small ($1/L_2 \gg \lambda_3 = g_3^2 N$[18]), we can use a dimensional reduction to the two-dimensional torus $S^1_\beta \times S^1_L$: owing to the antiperiodic boundary condition along L_2, all fermions would acquire a mass proportional to $1/L_2$ and we can ignore them.[19]

One would, thus, expect the gravitational system, for small L_2, to describe a dual of (3) with $D = 8$. Unfortunately, however, the gravity solutions are not valid in the small L_2 region ($L_2 \ll 1/\lambda_3$) since stringy corrections become important (see Appendix D 1 b).[20] In case of $L_2 \gg 1/\lambda_3$, since the fermions are not decoupled, the D2 brane theory will depend on the boundary conditions of fermions along the t and x_1 directions. There are four

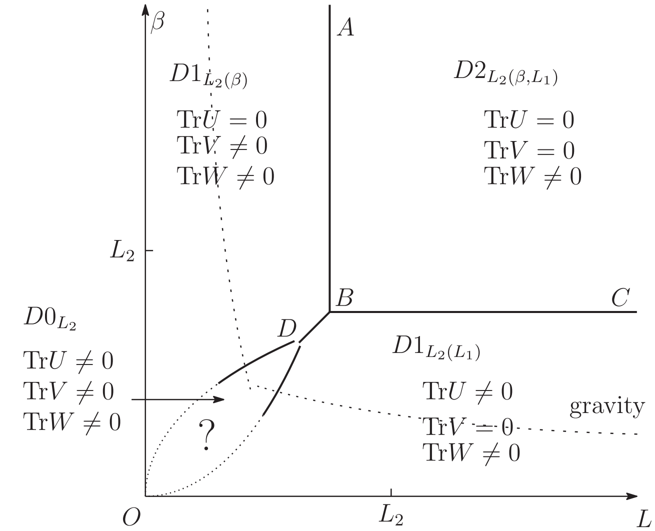

FIG. 5. Conjectured phase structure of the gauge theory from the gravity analysis. We used a large L_2 and the (P,P,AP) spin structure of the fermions on the three-dimensional torus (with AP boundary condition on the Scherk-Schwarz (SS) circle). TrW is the Polyakov loop operator along the SS circle (D16). The gravity analysis is reliable only in the region above the dotted line. The transitions in this diagram are predicted to be first order phase transitions. (See Appendix D 4).

choices of boundary conditions: (AP,AP), (AP,P), (P,AP), (P,P), where P denotes the periodic boundary condition and AP denotes the antiperiodic one.[21] Phase diagrams of the gravity theories for different spin structures are worked out in Appendix D and presented in Figs. 5, 7, and 8. The salient features are:

(i) The phase structures in the gravity analysis depend on the boundary conditions.

(ii) Only the gravity analysis with (P,P) boundary condition is reliable as a prediction for gauge theory through the arguments in Appendix D 4. The phase structure in this case is shown in Fig. 5. It predicts the second joining pattern in Fig. 4.

(iii) The phase transitions in the gravity description in Fig. 5 are Gregory-Laflamme (type) transitions [49–51] and are expected to be of the first order, at least for large L_2 [5,23].

(iv) The gravity analysis for small β and L is not reliable.

Comparing Figs. 4 and 5, we can see that both diagrams share some common features. Both have four phases in similar parameter regions. In particular, the behavior of the transition lines for large β and large L is the same. The line BC in Fig. 5 is independent of L. This is consistent with large N volume independence [9,10,52], since Tr$V = 0$ on both sides of BC. Similar remarks apply to the line AB as well.

[18]This implies $1/L_2 \gg \sqrt{\lambda_2}$.

[19]In fact, even the scalars would acquire a mass at one-loop, as in [22]. However, unlike in [22], the scalar mass does not become infinite as $L_2 \to 0$. From the 2d gauge theory perspective, the scalar mass renormalization due to fermion loops schematically goes as $m_Y^2 = g_2^2 N \int d^2 p \frac{1}{(m)(p+m)} = \lambda_2 \frac{1}{m} \Lambda = \lambda_2$, where we have used a fermion mass $m = 1/L_2$ and an uv cutoff for the 2d theory $\Lambda = 1/L_2$. For a more precise calculation, see Appendix A. Since the scalars remain light compared to the KK scale, we must keep them in the Lagrangian as in (3).

[20]This is a common problem in the construction of holographic duals of nonsupersymmetric gauge theories. Since the gauge theory coupling constant λ_3 is greater than the KK scale ($1/L_2$) in the region of validity of gravity, the gravity description has been likened (cf. [26], p. 196–197) to strong coupling lattice gauge theory, the small L_2 limit being regarded as analogous to the continuum limit. Interesting results, including the qualitative predictions in [22], and results in AdS/QCD, have been obtained using this philosophy. We will use the small L_2 extrapolation of our gravity results in this spirit.

[21]The gravity calculation with $\beta = L$ in the (P,P) case has been studied in [5,25].

In the small β, L region too, the two phase diagrams share similarities. In Fig. 5, two phase transition lines emanate from the point D towards low values of β, L. However, it is not clear from the gravity analysis how to continue towards the origin. On the other hand, in Fig. 4 the region near the origin O can be computed reliably and the two (double) lines OD_1 and OD_2 can be identified as a continuation of the two phase transition lines mentioned above. We should note that the phase structure in the small β, L region of Fig. 4 can be calculated from gauge theory even at strong coupling, up to $\tilde{\lambda}' \lesssim \lambda_{\max}$ where $\lambda_{\max} = L/\beta^3$ for $\beta \ll \beta_{\rm cr}$, and $\lambda_{\max} = \beta/L^3$ for $L \ll L_{\rm cr}$; as λ grows stronger, the calculable region becomes narrower.

In addition to the above similarities, various details of the phases in Fig. 4 and 5 are also similar. Recall that the phases in the gauge theory are characterized by three solutions: uniform, nonuniform and gapped. Correspondingly, three solutions (uniform black string, nonuniform black string and localized black hole) play a key role in the discussion of Gregory-Laflamme transitions in gravity. For large L, the free energy of these solutions in the gauge theory are related as shown in Fig. 3. A similar relation has been found in gravity [53], in the case where the GL transition is of first order. On the other hand, if the GL transitions are of higher order, it consists of two transitions: a transition between a uniform black string and a nonuniform one, and another transition between the nonuniform black string and a localized black hole [50]. This is precisely similar to the higher order phase transitions in the gauge theory, which we have observed in the small L case.

An important consequence of the gravity analysis is that we can guess how the phase transitions in Fig. 4 are connected. In particular, it indicates that there is no direct transition between $\mathrm{Tr}U = \mathrm{Tr}V = 0$ and $\mathrm{Tr}U \neq 0$, $\mathrm{Tr}V \neq 0$ phase. In [5], it was pointed out that this property has also been observed in large N pure Yang-Mills theories on four- and three-dimensional tori in the lattice calculations of [2,54,55]. Thus, the gravity analysis is in agreement with the lattice calculation. More details of the lattice calculation are presented in Sec. VI.

In summary, the full phase diagram of the two-dimensional gauge theory (3) may be obtained by combining the results from gauge theory and gravity. The result would be given by Fig. 4 with the second joining possibility.[22]

VI. RELATION TO OTHER WORKS

In this section, we detail some of the remarks made in the Introduction regarding previous works.

A. Comparison with lattice studies

Large N Yang-Mills theories on tori have been studied using lattice methods in [2,4,54,55], in $d = 3$ and four dimensions. Reference [4] contains a nice summary of these works. We describe some of the salient features below (see also Fig. 6).

(a) If we start from $d = 4$ pure Yang-Mills theory on a Euclidean torus T^4 with $L_3 < L_2 < L_1 < L_0$,[23] then for all radii large enough the center symmetry Z_N^4 (see footnote 3) is unbroken and all the Wilson loops W_μ vanish. This phase is called the 0_c phase. In this completely unbroken phase, the thermodynamics in the large N limit does not depend on any one of the lengths L_μ [9–11].

(b) As L_3 is decreased, below a certain value L_3^c there is a phase transition to a new phase where the center symmetry is broken to Z_N^3 and W_3 develops a nonzero expectation value. The other Wilson loops W_0, W_1 and W_2 still vanish. This phase is called the 1_c phase in which there is no dependence on the lengths L_μ, $\mu = 0, 1, 2$ which characterize the directions of unbroken center symmetry.

(c) If L_2 is now decreased, maintaining $L_2 > L_3$, a new phase 2_c appears below L_2^c (which is a function of L_3) where W_2 becomes nonzero. The center symmetry is broken to Z_N^2, with nonzero values of W_2, W_3 while W_0, W_1 still vanish.

(d) Proceeding similarly, a phase 3_c is reached when L_1 is reduced below a critical value $L_1^c(L_2, L_3)$, and the phase 4_c are reached when, finally, L_0 is reduced below $L_0^c(L_1, L_2, L_3)$.

(e) Thus, $d = 4$ pure YM theory (with $L_3 < L_2 < L_1 < L_0$) exhibits a cascade of transitions

$$0_c \to 1_c \to 2_c \to 3_c \to 4_c.$$

(f) In the case of $d = 3$ pure Yang-Mills theory (with $L_2 < L_1 < L_0$), the sequence of transitions works similarly, leading to a cascade

$$0_c \to 1_c \to 2_c \to 3_c.$$

(g) It was found in [2,54] that the cascade of transitions persists even when all radii are the same. For example, in case of the system in (f) with $L_1 = L_2 = L_3 = L$, for high enough L all $W_\mu = 0$; as L is reduced below a certain critical value L_c, only one of the W_μ's picks up a nonzero value [2], and the 3D cubic symmetry group spontaneously

[22] The extrapolation involved in this conclusion has additional support from the lattice calculations mentioned above.

[23] Since all directions are equivalent in the Euclidean space, the ordering chosen here is arbitrary and all arguments below can be repeated with any other ordering.

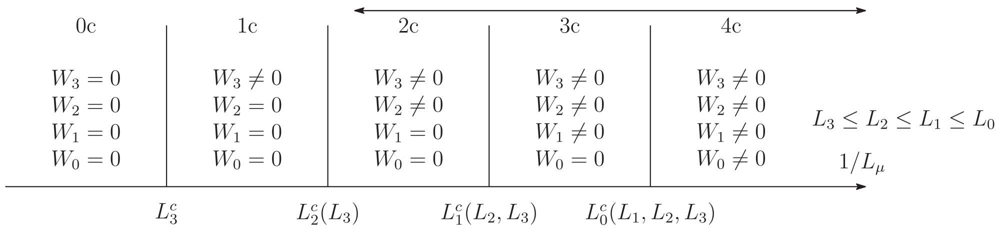

FIG. 6. Cascade of phase transitions for pure Yang-Mills theory on a T^4 (adapted from [4]; see the points (a)-(e) above for more details). Our results in this paper, for the theory (3) with $D = 2$, describe the indicated phases 2_c, 3_c and 4_c. The $0_c \to 1_c$ transition is found to be first order from lattice studies in [56]; the $2_c \to 3_c$ transition is found to be first order from our analysis; the $3_c \to 4_c$ transition for an asymmetric torus is found in our analysis to be a double (2nd order + 3rd order) transition for an appropriate parameter regime (see Fig. 4), although, it can be a single first-order transition at other regimes [6,60].

breaks down to the symmetry group appropriate to a square lattice.

(h) Generally speaking, it was found in these works that the Wilson lines W_μ change from zero to nonzero one by one; two or more Wilson lines never simultaneously change from zero to nonzero values.

(i) *Order of phase transitions:*[24] There is ample evidence that the first of the cascade of transitions $Z_N^{d+D} \to Z_N^{d+D-1}$ is first order. In the case of $0_c \to 1_c$ transitions in four-dimensional Yang-Mills theories on T^4, such evidences are presented directly in [56] and indirectly, assuming large N volume independence, in [57–59]. Evidences for the first order nature of the $0_c \to 1_c$ and $1_c \to 2_c$ phase transitions have been presented for Yang-Mills theory on T^3 in [60], which indicates that the first two transitions $Z_N^{d+D} \to Z_N^{d+D-1} \to Z_N^{d+D-2}$ are also first order. Our gauge theory analysis presents analytic evidence that the first order nature continues till the transition $Z_N^2 \to Z_N^1$ (which is $2_c \to 3_c$ in the notation of pure Yang-Mills theory on T^4), whereas the last transition $Z_N \to 1$ in which the center symmetry is completely broken, occurs (in the parameter region of Sec. III[25]) in two steps through a second and a third order phase transitions. The last statement, first derived in [6], is corroborated by the numerical work in [46].

Let us compare the above with the phase diagram in Fig. 4, which describes phases of the theory (3). Note that the theory (3) with $D = 2$[26] is precisely the one obtained after the steps (a)-(b) described above, in which we reduce a $d = 4$, $D = 0$ theory (pure YM theory in four dimensions) on two small circles of length L_2, L_3. To make the correspondence more explicit, we identify $L_1 = L$, $L_0 = \beta$, $W_1 = \mathrm{Tr}V$, $W_0 = \mathrm{Tr}U$. It is easy to see that the phase transitions in the $L < \beta$ region of Fig. 4 precisely correspond to the phase transitions described in (c)-(d) above.[27] The top right part of Fig. 4 (above AB_1B_2C) represents the 2_c phase. The region above the line OD_1B_2A (or its mirror image: the region to the right of the line OD_2B_2C) corresponds to the 3_c phase. The enclosed region OD_1D_2O corresponds to the 4_c phase. The phase transition across AB_1 from right to left corresponds to the transition $2_c \to 3_c$; the phase transition across OD_1[28] from above corresponds to $3_c \to 4_c$ (see Fig. 6).

The comments (g)-(h) above have a direct bearing on the possible joining pattern in Fig. 4. Out of the three possible joining patters shown in the insets, the first and the third patterns allow a direct transition $2_c \to 4_c$ and are, hence, inconsistent with the comment (h). Thus, consistency with the lattice results described in this subsection uniquely pick up the second joining pattern. As we showed in Sec. V, the same joining pattern is also picked up uniquely in Fig. 5 through the analysis of the gravity dual.

A more quantitative comparison of our work with the above lattice studies is left for the future.

We should mention another important lattice study [61] which deals with super Yang-Mills theories in $d = 2$ and is closely related to the work presented here and in [6]. In parameter ranges where the two theories coincide, our phase diagrams agree (see Sec. 5 of [61]). See also related numerical works about the center symmetry breaking in super Yang-Mills [62,63].

B. Comparison with earlier analytical studies with massive adjoint scalars

Reference [3] considers the theory (3) in the limit $m \gg \lambda_2^{1/2}$. Our Fig. 4 is similar to Fig. 13 of [3], except

[24]We thank Rajamani Narayanan for pointing out some references in this paragraph.

[25]In other parameter regions, $3_c \to 4_c$ can be a single first order phase transition [6,60].

[26]We will assume that the essential features of the large-D calculation which led to this phase diagram remain valid for $D = 2$. This was certainly true in the $d = 1$ case discussed in [6].

[27]The $\beta < L$ region is the mirror image; it corresponds to the sequence similar to (c)-(d) resulting from an ordering $L_0 < L_1$.

[28]We are treating the nonuniform phase as part of the 4_c phase here.

that our figure is obtained for any mass (including $m = 0$) where their figure is for the large mass limit. The reason for the agreement is the appearance of a dynamical mass Δ for the adjoint scalars in our model, as we have explained above.

In Fig. 14 of [3], an interpolation between small and large radii is proposed on the basis of some analytical estimates for the intermediate radii. Our Fig. 5, although similar to this figure, differs in one crucial respect. The phase transition line BC in our figure is horizontal throughout, as it must be according to large N volume independence arguments [9,10]. Since the line BC is entirely in the $\mathrm{Tr}V = 0$ phase, the transition temperature β_c cannot depend on L; hence BC must be horizontal. This property is violated by the corresponding line (the intermediate radius segment) of Fig. 14 in [3], which should have been horizontal according to the above argument.

C. Comparison with Yang-Mills theories on different topologies

We have found that the nature (in particular, *order*) of the confinement/deconfinement type transition at β_c in the two-dimensional gauge theory (3) at a fixed radius L depends on the value of L. Since this theory can be obtained from a pure Yang-Mills theory on a small $T^D \times S^1_L \times S^1_\beta$, it is interesting to compare this result with Yang-Mills theories on compact spaces with other topologies. We present such a comparison in Table I.[29]

Because of the difficulty of the analysis of Yang-Mills theory, only weakly coupled Yang-Mills theories on S^2 and S^3 [64,65] have been studied. In these cases, all the spatial components of the gauge field have a mass proportional to $1/R$, where R is the radius of the sphere. These massive gauge fields can be integrated out perturbatively if the radius is sufficiently small ($R\Lambda_{\mathrm{QCD}} \ll 1$). References [64,65] derived effective potentials for A_0 up to three-loop order and found the transition in the S^3 case to be first order [64]. On the other hand, the transition in the S^2 case consists of second and third order transitions as we found in the small T^D case [65]. Note that the higher order transitions for small S^2 is expected to change to a first order transition in a strong coupling regime according to lattice studies [66].

Thus, the nature of the transition depends not only on the size but also on the topology of the compact space. It would be interesting to understand the origin of these differences.

VII. CONCLUSIONS

In this work, we have computed the phase diagram of two-dimensional Yang-Mills theory with adjoint scalars (3), which can be obtained from a KK reduction of a higher-dimensional pure Yang-Mills theory. We treated the case of massless adjoint scalars in detail, outlining the generalization to arbitrary nonzero mass in Appendix C, and found the phase diagram in Fig. 4. At large spatial radius, there is a first order confinement/deconfinement phase transition, whereas at small spatial radius, there are two closely spaced phase transitions: (a) a second order phase transition from the "confined" phase to a "nonuniform" phase (nonuniform eigenvalues of the Polyakov line), followed by (b) a third order phase transition from the "nonuniform" phase to a "gapped" phase. Our calculations, based on the large-D method [6], provide an analytical derivation of the dependence of the thermodynamic behavior on the size of the spatial box, which is anticipated on the basis of lattice studies and gauge/gravity duality.

We have also considered the phase transitions in the gauge theory from the viewpoint of a gravity dual, based on a scaling limit of Scherk-Schwarz compactification of a D2 brane on a 3-torus. Although there is no overlapping region of validity of the gauge theory and gravity descriptions, the analysis of the gravity dual leads us to conjecture a certain specific completion of the phase diagram in the gauge theory, as in Fig. 5. In performing this analysis, we encountered an inherent problem with the holographic analysis, namely, a dependence of the physics on the fermion boundary conditions, which was absent in the gauge theory description (see Appendix D). Indeed, this problem is related to a more general problem in the holographic description of QCD [67]. We discuss this problem further in [68].

We matched our findings from gauge theory regarding the *order* of various phase transitions with those from a gravity analysis in Sec. V and with those from lattice studies in Sec. VI.

Note that the method of integrating out the adjoint scalars using a $1/D$ expansion works equally well in higher-dimensional ($d \geq 3$) gauge theories (B1), leading to an effective action for the gauge field as shown in (B7). However, it is difficult to evaluate the dynamics of this model because of the existence of dynamical gluons. This is a crucial difference from the lower-dimensional cases ($d = 0, 1, 2$). In addition, the d-dimensional model (B1)

TABLE I. Confinement/deconfinement type transitions in pure Yang-Mills theories on $S^1_\beta \times \mathcal{M}$. Here, "small S^1" and "small T^D" refer to sizes small enough to ensure (a) that the Z_N symmetries in the S^1 and T^D directions, respectively, are broken, and (b) that all the KK modes can be integrated out. "Large S^1" ensures that the Z_N symmetry along the S^1 is not broken.

$\mathcal{M}$	Type of phase transition
Small $T^D\times$ small S^1	2nd + 3rd
Small $T^D\times$ large S^1	1st
Small S^2	2nd + 3rd
Small S^3	1st

[29]In order to apply $1/D$ expansion, we need $D \geq 1$ in the small $T^D\times$ small S^1 case and $D \geq 2$ in the small $T^D \times$ large S^1 case.

typically appears through a KK reduction of a $d+D$-dimensional (super) Yang-Mills theory, but for $d \geq 3$ the mass of the adjoint scalars induced from loops of KK modes is large (see Appendix A); hence, the contribution of the adjoint scalars may be not relevant for $d \geq 3$.

The investigations in the present paper were partly motivated by a desire to understand a gauge theory dual to a dynamical Gregory-Laflamme transition. The considerations in this paper provide a step towards understanding this issue; details of this will appear elsewhere [27].

ACKNOWLEDGMENTS

We would like to thank Gyan Bhanot, Sumit Das, Saumen Datta, Avinash Dhar, Sourendu Gupta, Shiraz Minwalla, Sreerup Raychaudhuri and Mithat Unsal for useful discussions. We would also like to thank Pallab Basu, Manavendra Mahato and Spenta Wadia for numerous interactions and collaboration at an early stage, and Sumit Das, Avinash Dhar, Shiraz Minwalla, Rajamani Narayanan, Vasilis Niarchos and Mithat Unsal for comments on the draft and for pointing out important references. G. M. would like to thank the University of Kentucky, Lexington for hospitality where part of the work was done, and the seminar audiences in Lexington, and at the String Theory meeting ISM 2011 in Puri, for useful interactions. T. M. would like to thank KEK for hospitality where part of the work was done. This work is partially supported by Regional Potential program of the E.U. FP7-REGPOT-2008-1: CreteHEPCosmo-228644, and by Marie Curie Contract No. PIRG06-GA-2009-256487.

APPENDIX A: MASS FOR Y^I FROM ONE-LOOP OF THE KK MODES

If we consider a $d+D$-dimensional Yang-Mills on T^{d+D} (1) and consider a dimensional reduction by taking the radii of T^D to be small, we will classically obtain a d-dimensional gauge theory coupled to D massless adjoint scalars. However, if we consider quantum effects, the action would be modified. One of the relevant corrections is that the adjoint scalars would acquire mass as in (B1). In this appendix, we evaluate the mass at a one-loop level.[30]

Starting from the $d+D$-dimensional action (1), we can derive a one-loop effective action for the constant diagonal components of $A^\mu = (a_1^\mu, \cdots, a_N^\mu)$ by integrating out all the other modes [1,3,69],

$$S_{\rm eff} = -\left(\prod_{\mu=0}^{d+D-1} L_\mu\right)\frac{d+D-2}{2}\frac{\Gamma[(d+D)/2]}{\pi^{(d+D)/2}} \times \sum_{i,j}\sum_{\{k_\mu\}\neq\{0\}} \frac{\exp[i\sum_\nu k_\nu L_\nu (a_i^\nu - a_j^\nu)]}{(\sum_\nu k_\nu^2 L_\nu^2)^{(d+D)/2}}. \tag{A1}$$

Here, the sum $\sum_{\{k_\mu\}\neq\{0\}}$ includes all integers k_μ except $k_0 = \cdots = k_{d+D-1} = 0$. Let us now take L_μ ($\mu = 0, \cdots, d-1$) large and L_I ($I = d, \cdots, d+D-1$) small and derive a low-energy effective theory by using this expression. Gauge invariance implies that the effective action in this situation will be given by

$$\begin{aligned} S_d = &\int_0^\beta dt \prod_{i=1}^{d-1}\int_0^{L_i} dx^i\, \mathrm{Tr}\Big(\frac{1}{4g_d^2}F_{\mu\nu}^2 + \sum_{I=1}^{D}\frac{1}{2}(D_\mu Y^I)^2 \\ &- \sum_{I,J}\frac{g_d'^2}{4}[Y^I, Y^J][Y^I, Y^J]\Big) \\ &- \int_0^\beta dt \prod_{i=1}^{d-1}\int_0^{L_i} dx^i \Big(\prod_{I=1}^{D} l_I\Big)\frac{d+D-2}{2} \\ &\times \frac{\Gamma((d+D)/2)}{\pi^{(d+D)/2}} \sum_{\{k_I\}\neq\{0\}} \frac{|\mathrm{Tr} e^{ig_d\sum_J k_J l_J Y^J}|^2}{(\sum_J k_J^2 l_J^2)^{(d+D)/2}}. \end{aligned} \tag{A2}$$

Here, we have rewritten $A_{d+I-1} = g_d Y_I$ and $L_{d+I-1} = l_I$. g_d and g_d' are the same as g and g' of (3); they satisfy $g_{d+D}^2/\prod_{I=1}^D l_I = g_d^2 = g_d'^2$ at a physical scale $\mu \gg 1/l_I$ (*cf.* (15)).

If l_I are small and the long string modes are suppressed (see footnote 4), we can treat Y^I perturbatively. Then we can expand the exponentials in (A2) and obtain a quadratic term in Y as

$$g_d^2 N\Big(\prod_{I=1}^{D} l_I\Big)(d+D-2)\frac{\Gamma[(d+D)/2]}{\pi^{(d+D)/2}} \times \sum_{\{k_I\}\neq\{0\}} \frac{k_I^2 l_I^2}{(\sum_J k_J^2 l_J^2)^{(d+D)/2}}\frac{\mathrm{Tr}(Y^I)^2}{2}. \tag{A3}$$

Other interaction terms from the exponential would be suppressed by small l_I. If we take all the l_I to have a common value $l_{KK} = 1/M_{KK}$, we obtain a mass for Y^I as

$$m^2 = g_d^2 N M_{KK}^{d-2}(d+D-2)\frac{\Gamma[(d+D)/2]}{\pi^{(d+D)/2}} \times \sum_{\{k_I\}\neq\{0\}}\frac{1}{D}\frac{1}{(k_1^2+\cdots+k_D^2)^{(d+D)/2-1}}. \tag{A4}$$

This sum would diverge for $d \leq 2$ and hence needs to be regulated, e.g. by using a prescription $(\vec{k})^2 \equiv k_1^2 + \cdots + k_D^2 \leq (\Lambda_{UV}/M_{KK})^2$, where Λ_{UV} is a cutoff scale.[31] This would imply a nontrivial RG flow of the mass. Let us first consider the case of $d=2$. For $\Lambda_{UV} \gg M_{KK}$, the regulated sum (A4) approximately gives $m^2(\Lambda_{uv}) = Ag_2^2 N \log(\Lambda_{uv}/M_{KK})$, where A is a numerical constant.

[30] We do not use the large-D limit in this appendix.

[31] An ultraviolet cutoff typically breaks gauge symmetry. The calculation discussed here can be repeated avoiding such problems, by using dimensional regularization [7].

Let us choose a renormalization scale $\mu \gtrsim O(M_{KK})$. We can then define a renormalized mass at the scale μ as

$$\bar{m}^2 \equiv m^2(\Lambda_{uv}) - Ag_2^2 N \log(\Lambda_{uv}/\mu) = A'\lambda_2, \qquad \text{(A5)}$$

where $A' = A\log(\mu/M_{KK})$, $\lambda_2 = g_2^2 N$. Note that the running of the mass will stop below $\mu < M_{KK}$.

For $d = 1$, a similar analysis gives

$$\bar{m}^2 \sim \lambda_3/M_{KK}. \qquad \text{(A6)}$$

For $d \geq 3$, the sum in (A4) is convergent, leading to $m \sim \lambda_d^{1/2} M_{KK}^{(d-2)/2}$ which is much larger than the typical QCD scale, e.g. for $d = 3$ the QCD scale is $O(\lambda_3)$ whereas the adjoint mass is $O(\lambda_3^{1/2} M_{KK}^{1/2})$. Thus, if M_{KK} is large, the adjoint scalars will not contribute to the QCD dynamics. It means that only the d-dimensional gauge field dominates the dynamics.[32]

So far, we have considered the mass correction from the KK modes in pure Yang-Mills theory. We can extend this calculation to the KK reduction of supersymmetric theories with a Scherk-Schwarz compactification, e.g. to the derivation of (3) with $D = 8$ from the D2 theory. In this case, we need to evaluate the contribution of loops of adjoint scalars as well as fermions. However, it can be shown that we obtain a similar mass $\sim O(\lambda_d^{1/2} M_{KK}^{(d-2)/2})$ even in this case [3].

APPENDIX B: DERIVATION OF EFFECTIVE POTENTIAL (10)

In this appendix, we show the derivation of the effective action (11) from (10) with the assumptions (a) and (b) below (10). We can evaluate (10) in a general d-dimensional gauge theory, described by the action

$$S = \int_0^\beta dt \prod_{i=1}^{d-1} \int_0^{L_i} dx^i \,\mathrm{Tr}\Big[\frac{1}{4g^2} F_{\mu\nu}^2 + \sum_{I=1}^{D} \frac{1}{2}(D_\mu Y^I)^2 + \frac{m^2}{2} Y^{I2} - \sum_{I,J} \frac{g'^2}{4}(Y^I, Y^J)(Y^I, Y^J)\Big]. \qquad \text{(B1)}$$

This model can be identified with (A2) if we take L_I small and choose the mass and couplings appropriately. We will first discuss the general d-dimensional case and apply the results to $d = 2$ later.

Let us first set $m = 0$. Then, through a similar calculation as in Sec. II A, we obtain a generalization of (10) (the calculation closely follows [3]). In this section, we will use the more general notation (L_0, L_1) for (β, L).

$$\begin{aligned}\delta S[A, \Delta] &= \frac{D}{2} \log\det(-D_\mu^2 + \Delta^2) \\ &= \frac{D}{2} \mathrm{Tr} \sum_{\{n_\mu\}} \log\Big(\sum_{\mu=0}^{d-1}\Big(\frac{2\pi n_\mu}{L_\mu} + A_\mu\Big)^2 + \Delta^2\Big) \\ &= \frac{D}{2} \frac{L_0 \cdots L_{d-1}}{(2\pi)^d} \mathrm{Tr}_{adj} \sum_{\{k_\mu\}} P_{\{k_\mu\}}(\Delta, \{L_\mu\}) e^{i\sum_\mu k_\mu L_\mu A_\mu},\end{aligned} \qquad \text{(B2)}$$

where $P_{\{k_\mu\}}$ is

$$\begin{aligned}P_{\{k_\mu\}}(\Delta, \{L_\mu\}) &= \int_0^{2\pi/L_0} da_0 \cdots \int_0^{2\pi/L_{d-1}} da_{d-1} \sum_{\{n_\mu\}} \log\Big(\sum_{\mu=0}^{d-1}\Big(\frac{2\pi n_\mu}{L_\mu} + a_\mu\Big)^2 + \Delta^2\Big) e^{-i\sum_\mu k_\mu L_\mu a_\mu} \\ &= \sum_{\{n_\mu\}} \int_{n_0}^{n_0 + 2\pi/L_0} da_0 \cdots \int_{n_{d-1}}^{n_{d-1} + 2\pi/L_{d-1}} da_{d-1} \log\Big(\sum_{\mu=0}^{d-1} a_\mu^2 + \Delta^2\Big) e^{-i\sum_\mu k_\mu L_\mu a_\mu} \\ &= \int_{-\infty}^{\infty} da_0 \cdots \int_{-\infty}^{\infty} da_{d-1} \log\Big(\sum_{\mu=0}^{d-1} a_\mu^2 + \Delta^2\Big) e^{-i\sum_\mu k_\mu L_\mu a_\mu}.\end{aligned} \qquad \text{(B3)}$$

Let us now evaluate $P_{\{k_\mu\}}$ in the $\{k_\mu\} = \{0\}$ and $\{k_\mu\} \neq \{0\}$ cases separately. In the $\{k_\mu\} \neq \{0\}$ case, $P_{\{k_\mu\}}(\Delta, \{L_\mu\})$ becomes,

[32] For $d = 2$, the mass of the adjoint scalar from the KK modes is finite ($O(\lambda_2)$) but the dynamical mass Δ is (logarithmically) larger than λ_2 [see (19)]. Hence, one may naively think that the adjoint scalar would be irrelevant as for $d \geq 3$. However, this is not correct [3], since the phase structure of the 2d pure Yang-Mills on T^2 is trivial and is always confined. Therefore, the contribution of the (logarithmically) heavy adjoint scalars is important in the two-dimensional gauge theory (3).

$$\begin{aligned} P_{\{k_\mu\}}(\Delta,\{L_\mu\}) &= \int_{-\infty}^{\infty} da_0 \cdots \int_{-\infty}^{\infty} da_{d-1} \log\Big(\sum_{\mu=0}^{d-1} a_\mu^2 + \Delta^2\Big) e^{-i\sum_\mu k_\mu L_\mu a_\mu} \\ &= \int_{-\infty}^{\infty} da_0 \cdots \int_{-\infty}^{\infty} da_{d-1} \lim_{\epsilon\to 0}\Big[-\log\epsilon - \gamma - \int_\epsilon^\infty \frac{d\alpha}{\alpha} e^{-(\sum_\mu a_\mu^2+\Delta^2)\alpha}\Big] e^{-i\sum_\mu k_\mu L_\mu a_\mu} \\ &= -\pi^{d/2}\int_0^\infty \frac{d\alpha}{\alpha^{d/2+1}} e^{-\Delta^2\alpha-(1/4\alpha)\sum_\mu (k_\mu L_\mu)^2} = -\frac{2(2\pi\Delta)^{d/2}}{\Big(\sqrt{\sum_\mu (L_\mu k_\mu)^2}\Big)^{d/2}} K_{d/2}\Big(\Delta\sqrt{\sum_\mu (L_\mu k_\mu)^2}\Big) \\ &= -\frac{2(2\pi\Delta)^{d/2}}{\Big(\sqrt{\sum_\mu (L_\mu k_\mu)^2}\Big)^{(d+1)/2}}\sqrt{\frac{\pi}{2\Delta}}\exp\Big(-\Delta\sqrt{\sum_\mu (L_\mu k_\mu)^2}\Big) + \cdots, \end{aligned} \tag{B4}$$

where $K_{d/2}$ is the modified Bessel function of the second kind and we have used $K_a(z) = \sqrt{\pi/2z}e^{-z} + \cdots$ for large z in the last equation.

For $\{k_\mu\} = \{0\}$, we find

$$\begin{aligned} P_{\{0\}}(\Delta,\{L_\mu\}) &= \int_{-\infty}^{\infty} da_0 \cdots \int_{-\infty}^{\infty} da_{d-1} \log\Big(\sum_{\mu=0}^{d-1} a_\mu^2 + \Delta^2\Big) \\ &= \int_0^\Lambda da\Omega_d a^{d-1}\log(a^2+\Delta^2), \end{aligned} \tag{B5}$$

where $\Omega_d = 2\pi^{d/2}/\Gamma(d/2)$ is the surface area of the d-dimensional unit sphere and Λ is a cutoff.

Finally, we turn on the mass term. In this case, we can obtain the results by replacing $\Delta \to \sqrt{\Delta^2 + m^2}$ in (B4) and (B5). Note that the assumption (a) and (b) below (10) should be modified accordingly.

1. Effective action for $d = 2$

We now consider the special case of $d = 2$. In this case, we can evaluate $P_{\{0\}}$ as

$$\begin{aligned} P_{\{0\}}(\Delta,\beta,L) &= 2\pi\int_0^\Lambda daa\log(a^2+\Delta^2) \\ &= -\pi\Lambda^2 + \pi(\Lambda^2+\Delta^2)\log(\Lambda^2+\Delta^2) \\ &\quad - \pi\Delta^2\log\Delta^2. \end{aligned} \tag{B6}$$

By using this result and (B4) to (B2), we obtain the effective action (11). Note that $\mathrm{Tr}_{\mathrm{adj}} e^{i(k\beta A_0 + lLA_1)}$ in (B2) becomes $|\mathrm{Tr}(U^k V^l)|^2$ by using the assumption (b).

2. Effective potential for higher-dimensional models

It is easy to generalize the derivation of the effective potential (20) for the two-dimensional gauge theory in Sec. II A to the d-dimensional gauge theory (B1) for large L_μ.[33] By using the results in the previous section, we obtain

$$\begin{aligned} S = \prod_{\mu=0}^{d-1}\int_0^{L_\mu} dx_\mu \Big(&\frac{1}{4g^2}\mathrm{Tr}F_{\mu\nu}^2 - \frac{DN^2}{(2\pi)^{(d-1)/2}} \\ &\times \sum_{\mu=0}^{d-1}\frac{(\Delta_0^2+m^2)^{(d-1)/4}}{L_\mu^{(d+1)/2}} e^{-\sqrt{\Delta_0^2+m^2}L_\mu}\Big|\frac{1}{N}\mathrm{Tr}e^{iL_\mu A_\mu}\Big|^2\Big) \\ &+ DN^2 L_0\cdots L_{d-1} \\ &\times\Big(-\frac{\Delta_0^4}{8\tilde\lambda'} + \frac{1}{2(2\pi)^d}P_0\Big(\sqrt{\Delta_0^2+m^2},\{L_\mu\}\Big)\Big). \end{aligned} \tag{B7}$$

Here, Δ_0 is defined as a solution of the saddle-point equation

$$\frac{\Delta^2}{2\tilde\lambda'} = \frac{\Omega_d}{(2\pi)^d}\int_0^\Lambda da\frac{a^{d-1}}{a^2+\Delta^2+m^2}. \tag{B8}$$

Note that we can always find a unique positive solution Δ_0 from this equation.

APPENDIX C: THE PHASE STRUCTURE OF MASSIVE MODEL.

In this appendix, we study the two-dimensional gauge theory (3) with a mass term for the adjoint scalars. As we mentioned in the introduction and elaborated in Appendix A, such a mass term generically arises from KK loops. We discuss here how the results of the massless case in Secs. II and III are modified. We will show that the mass does not change the qualitative nature of the phase structure.

1. Large L case

By using the results in B 2, we generalize the effective action for TrU (23) to the massive case. The resulting effective action is again given by (23) with different values of ξ and C:

$$\xi = \sqrt{\frac{\sqrt{\Delta_0^2+m^2}}{2\pi\tilde\lambda^2\beta^3}}e^{-\beta\sqrt{\Delta_0^2+m^2}}, \tag{C1}$$

[33]The $1/D$ expansion in the d-dimensional gauge theory (B1) in a high temperature region is considered in [37] also.

$$C(\tilde{\lambda}', \Delta_0) = \frac{\beta L \Delta_0^2}{8\pi}\left(1 + \frac{\pi\Delta_0^2}{\tilde{\lambda}'}\right) + \frac{\beta L m^2}{8\pi}\left(1 + \frac{2\pi\Delta_0^2}{\tilde{\lambda}'}\right). \tag{C2}$$

The dynamical mass Δ_0 is a solution of

$$\tilde{\lambda}' = \frac{2\pi\Delta_0^2}{\log(1 + \frac{\Lambda^2}{\Delta_0^2 + m^2})}. \tag{C3}$$

For large Λ, Δ_0 becomes

$$\Delta_0 = \sqrt{\frac{\tilde{\lambda}'}{2\pi} W\left(\frac{2\pi\Lambda^2}{\tilde{\lambda}'} e^{2\pi m^2/\tilde{\lambda}'}\right) - m^2}. \tag{C4}$$

Therefore, we can use the same analysis as in Sec. II B and obtain the same phase structure with the following modified transition temperatures

$$\beta_m = \frac{3}{2\sqrt{\Delta_0^2 + m^2}} W\left[\frac{2}{3(2\pi\xi_m^2)^{1/3}}\left(\frac{\Delta_0^2 + m^2}{\tilde{\lambda}}\right)^{2/3}\right]. \tag{C5}$$

Although the mass changes the explicit values of the transition temperatures and some other physical quantities, the qualitative nature of the phase structure is not modified, as we have mentioned.

Note that (C3) implies that Δ_0 becomes smaller as m increases for fixed $\tilde{\lambda}'$ and Λ. Therefore, for heavy mass, we can ignore the dynamical mass Δ_0 compared to m and our calculations reproduce the heavy mass QCD results in [3,14].

2. Small L case

If L is small enough in (3), we can integrate out all the nonzero momentum modes in the L direction (see footnote 4) and obtain a one-dimensional model (B1) with $d = 1$. In this case, the mass of the adjoint scalars induced at one-loop from the KK modes is proportional to $(\tilde{\lambda}_1 L)^{1/2}$ [see (A6)]. Hence, we can ignore it for small enough L and the results in [6] shown in Sec. III would still be valid. Although the contribution from the mass would be small, it may be valuable to confirm that the results in [6] are not modified qualitatively.

Starting from (B1) with $d = 1$, we obtain an effective potential through a similar calculation as in B 2,[34]

$$S_{\mathrm{eff}}(\Delta, \{u_n\})/DN^2 = -\frac{\beta\Delta^4}{8\tilde{\lambda}_1} + \frac{\beta\sqrt{\Delta^2 + m^2}}{2} + \sum_{n=1}^{\infty}\left(\frac{1}{D} - e^{-n\beta\sqrt{\Delta^2+m^2}}\right)\frac{|u_n|^2}{n}. \tag{C6}$$

[34] Contrary to the $d \geq 2$ case, the condition (a) and (b) below (10) are not required for a derivation of the effective action in the $d = 1$ case. Thus, the $1/D$ analysis would be valid as long as the effective dimensionless coupling $\tilde{\lambda}_1\beta^3$ does not scale with D.

Here, the third term is a contribution of the Vandermonde determinant [6]. Then, the saddle-point equation for Δ^2 becomes

$$\frac{\Delta^2}{\tilde{\lambda}_1} = \frac{1}{\sqrt{\Delta^2 + m^2}} + 2\sum_{n=1}^{\infty}\left(\frac{1}{\sqrt{\Delta^2 + m^2}} e^{-n\beta\sqrt{\Delta^2+m^2}}\right)|u_n|^2. \tag{C7}$$

The solution of this equation at low temperatures ($e^{-\beta\sqrt{\Delta^2+m^2}} \ll 1$) is

$$\Delta^2 = \Delta_0^2 + \frac{4\tilde{\lambda}_1\sqrt{\Delta_0^2 + m^2}}{3\Delta_0^2 + 2m^2} e^{-\beta\sqrt{\Delta_0^2+m^2}}|u_1|^2 + \cdots, \tag{C8}$$

where

$$\Delta_0^2 = \frac{m^2}{3}(f(m) + f(m)^{-1} - 1),$$
$$f(m) = \frac{1}{2^{1/3}m^2}\left[27\tilde{\lambda}_1^2 - 2m^6 + \sqrt{27\tilde{\lambda}_1^2(27\tilde{\lambda}_1^2 - 4m^6)}\right]^{1/3}. \tag{C9}$$

Note that, although $f(m)$ is a complex for $m^6 \geq 27\tilde{\lambda}_1^2/4$, Δ_0^2 is always real and positive. By substituting this solution to (C6), we obtain an effective action for u_n,

$$S_{\mathrm{eff}}(\{u_n\})/DN^2 = -\frac{\beta\Delta_0^4}{8\tilde{\lambda}_1} + \frac{\beta\sqrt{\Delta_0^2 + m^2}}{2} + a|u_1|^2 + b|u_1|^4 + \cdots, \tag{C10}$$

where

$$a = \left(\frac{1}{D} - e^{-\beta\sqrt{\Delta_0^2+m^2}}\right), \quad b = \frac{\beta\tilde{\lambda}_1}{3\Delta_0^2 + 2m^2} e^{-2\beta\sqrt{\Delta_0^2+m^2}}. \tag{C11}$$

One important fact is that b is always positive. It has been shown that, in this case, the confinement/deconfinement type transition always consists of the two transitions (2nd + 3rd) as in the massless case [6,20]. These critical temperatures are given by the solutions of $a = 0$ and $a/(2b) = -1/4$, respectively, and evaluated as

$$\beta_{c1} = \frac{1}{\sqrt{\Delta_0^2 + m^2}} \log D, \quad \beta_{c2} = \beta_{c1} - \frac{\tilde{\lambda}_1}{2D}\frac{\log D}{3\Delta_0^2 + 2m^2}. \tag{C12}$$

Therefore, as in the large L case, the qualitative nature of the phase transition is not modified by the mass term.[35]

Although we have evaluated only the leading order of the $1/D$ expansion in this section, the result does not change even if we include the next order.

APPENDIX D: PHASE STRUCTURE OF D2 BRANES ON A 3-TORUS

In this appendix, we consider the gravitational system of Sec. V in detail. We first review some generalities for Dp branes with arbitrary p.

1. Dp branes wrapped on $p+1$-Torus

a. The solutions

The geometry of a black Dp brane on a p-torus $x_i \in (0, L_i)$, $(i = 1, \cdots, p)$ in the Maldacena limit (assuming Euclidean time $t \in (0, \beta)$) [24] is given by

$$\begin{aligned} ds^2 &= \alpha'\bigg[F(u)\bigg(f(u)dt^2 + \sum_{i=1}^{p} dx_i dx_i\bigg) + \frac{du^2}{F(u)f(u)} \\ &\quad + G(u)d\Omega_{8-p}^2\bigg] \\ e^{\phi} &= \frac{(2\pi)^{2-p}\lambda_{p+1}}{N}[F(u)]^{(p-3)/2}, \qquad F(u) = \frac{u^{(7-p)/2}}{\sqrt{d_p\lambda_{p+1}}}, \\ G(u) &= \sqrt{d_p\lambda_{p+1}}u^{(p-3)/2}, \qquad f(u) = 1 - \left(\frac{u_0}{u}\right)^{7-p}, \\ d_p &= 2^{7-2p}\pi^{(9-3p)/2}\Gamma\left(\frac{7-p}{2}\right), \qquad \lambda_{p+1} = g_{p+1}^2 N, \end{aligned} \tag{D1}$$

where g_{p+1}^2 is the $p+1$-dimensional YM coupling, which, in the bulk theory, can be regarded as specifying a boundary condition for the dilaton field. The dimensionless YM coupling, defined by

$$g_{\rm eff}^2 = (g_{p+1}^2 N)u^{p-3} = (e^{\phi}N)^{2/(7-p)}, \tag{D2}$$

is given directly in terms of the dilaton; its dependence on u for $p \neq 3$ reflects the running of the gauge coupling. The scalar curvature is given by

$$\alpha' R = 1/g_{\rm eff}. \tag{D3}$$

Since time is Euclidean, $u \in (u_0, \infty)$. The smoothness condition at $u = u_0$ relates the inverse temperature β to u_0 as follows:

$$\frac{\beta}{2\pi} = \frac{\sqrt{d_p\lambda_{p+1}}}{7-p}u_0^{(p-5)/2}. \tag{D4}$$

The classical action of the black Dp brane is [5,23,24]

$$\begin{aligned} S/N^2 &= C_p\lambda_{p+1}^{(p-3)/(5-p)}L_1\cdots L_p\beta(-\beta^{-(2(7-p)/(5-p))} \\ &\quad + H_{\rm reg}(U)), \\ C_p &= \frac{5-p}{2^{11-2p}\pi^{(13-3p)/2}\Gamma((9-p)/2)a_p^{2(7-p)/(5-p)}}, \\ a_p &= \frac{7-p}{4\pi d_p^{1/2}}, \\ d_p &= 2^{7-2p}\pi^{(9-3p)/2}\Gamma\left(\frac{7-p}{2}\right)H_{\rm reg}(U) \\ &= \left(\frac{2a_p}{\sqrt{\lambda_{p+1}}}\right)^{2(7-p)/(5-p)}U^{7-p}, \end{aligned} \tag{D5}$$

which is evaluated by expressing the on-shell action as a regularized integral of $\sqrt{g}e^{-2\phi}R$ over the range $u_0 \le u \le U$.

In the following, we will also be interested in AdS solitons [22,70] which can be obtained from (D1) by moving the coefficient $f(u)$ from dt^2 to one of the x_i's, say to dx_p^2:

$$\begin{aligned} ds^2 &= \alpha'\bigg[F(u)\bigg(f(u)dx_p^2 + dt^2 + \sum_{i=1}^{p-1} dx_i dx_i\bigg) \\ &\quad + \frac{du^2}{F(u)f(u)} + G(u)d\Omega_{8-p}^2\bigg]. \end{aligned} \tag{D6}$$

The smoothness condition at $u = u_0$ now gives a condition analogous to (D4) where β is replaced by L_p. Thus, this solution has a contractible x_p-cycle (which wraps around a so-called "cigar" geometry on the (x_p, u) plane) along which the fermions must obey the antiperiodic (AP) boundary condition.

The regularized classical action evaluated on such a classical configuration is given by

$$\begin{aligned} S/N^2 &= C_p\lambda_{p+1}^{(p-3)/(5-p)}L_1\cdots L_p\beta\Big[-L_p^{-(2(7-p)/(5-p))} \\ &\quad + H_{\rm reg}(U)\Big], \end{aligned} \tag{D7}$$

where the notations are the same as before.

In a toroidal, Euclidean, spacetime, the time direction is on a similar footing as any other direction. Thus, the difference between the black brane and the solitonic

[35] Note that our results based on the $1/D$ expansion disagree with the results in [3]. Reference [3] studied the same model (C6) by using a large mass approximation, which is supposed to be valid if $\tilde{\lambda}_1/m^3 \ll 1$, up to three-loop order and concluded that the confinement/deconfinement transition in this model would be a single first-order transition. The difference would presumably arise from the fact that the $1/D$ expansion employed here evaluates the model in a nontrivial vacuum characterized by the nonzero Δ, whereas the large mass analysis of [3] is performed as a perturbation around the trivial vacuum. Numerical studies analogous to [46] but performed for massive adjoint scalars [47] should be able to provide further insight into this issue.

solution is only in the labeling of the contractible cycle (location of the "cigar" geometry). Hence, we will sometimes refer to both black branes as well as AdS solitons as just *Dp solutions*. In the following sections, we will consider different Dp solutions (with $p = 0, 1, 2$) which wrap on (are localized along) various cycles and, in order to distinguish them, we will use the following notation:

$Dp_{L_0(L_1,\ldots,L_p)}$ denotes a Dp solution which (i) has a contractible L_0 cycle (that winds around the "cigar") and (ii) wraps on the $L_1, \ldots, L_p$ cycles; this is a black brane. Similarly, $Dp_{L_p(L_0,L_1\ldots,L_{p-1})}$ denotes an AdS soliton in which the roles of t and x^p are flipped, as in (D6).

b. Validity of supergravity

The solutions described in the previous section are leading-order supergravity solutions. When we consider a black Dp brane solution (D1), the gravity analysis is reliable, if the parameters satisfy the following conditions [51]:

(1) The typical length scale of the black Dp brane near the horizon [see, e.g. (D3)] is given by $l = (\alpha'\sqrt{d_p\lambda_{p+1}}u_0^{(p-3)/2})^{1/2}$. In order to suppress stringy excitations, we should satisfy $l \gg \sqrt{\alpha'}$. From (D4), this condition is equivalent to

$$\lambda_{p+1}\beta^{3-p} \gg 1 \qquad (p \leq 5). \tag{D8}$$

(2) The mass of the winding mode along an L_i cycle is given by $M_{wi} = (\alpha' u_0^{(7-p)/2}/\sqrt{d_p\lambda_{p+1}})^{1/2}L_i/\alpha'$. In order to suppress the winding mode, we must have $M_{wi}l \gg 1$. This condition gives

$$\lambda_{p+1}^{1/2}L_i^{(5-p)/2} \gg \beta \qquad (p \leq 5). \tag{D9}$$

If this condition is violated and if the fermion on the brane satisfies the periodic (P) boundary condition along the L_i cycle, we can perform a T-duality along this direction and reassess the validity of supergravity in the dual frame.[36] After the T-duality, the black Dp solution becomes a smeared black $D(p-1)$ brane solution, which is composed of uniformly distributed $D(p-1)$ branes on the dual L_i cycle [23,71,72]. Then, the condition (D9) is replaced by $\tilde{M}_{wi}l \gg 1$, where $\tilde{M}_{wi} \equiv (\alpha' u_0^{(7-p)/2}/\sqrt{d_p\lambda_{p+1}})^{-1/2}(2\pi)^2/L_i$ is the mass of the winding mode on the dual cycle. This condition gives

$$L_i \ll \beta. \tag{D10}$$

Note that the first condition (D8) does not change under the T-duality (the value of the classical action is also invariant).

If, instead of a black Dp brane, we consider a solitonic solution which is obtained from the black brane by flipping $t \leftrightarrow x_i$, then the conditions for the validity of supergravity are simply obtained by replacing β and L_i in the above conditions.

We will discuss these criteria below in some detail in the parameter regime of interest.

2. Phase transitions of the Dp solutions

Using the on-shell classical actions (D5) and (D7), we can determine various phase transitions [5,25,26], as we will show now.

a. GL transition

The Gregory-Laflamme (GL) transition [49–51] was originally found in the context of black rings in $D \geq 5$ which were found to be unstable unless wrapped on a sufficiently small circle. In the context of black p-branes, the GL instability shows up as follows [23,71,72]. Suppose a black p-brane is wrapped on a circle of length L_1, along which the fermion satisfies the periodic boundary condition. If L_1 is so small that it violates (D9), we need the T-dualized description in terms of a uniformly smeared black $(p-1)$-brane on the dual circle of length $L_1' = (2\pi)^2/L_1$. If L_1' is large enough, the smeared black $(p-1)$-brane undergoes a GL transition leading to a black $p-1$ brane localized on the dual cycle. The transition can be studied dynamically, as well as thermodynamically. To study the latter, let us interpret (D5) without the regulator term (see Eq. (9) of [24]) as the Euclidean action (above extremality) of the smeared black $(p-1)$-brane:

$$S_p/N^2 = -C_p\lambda_{p+1}^{(p-3)/(5-p)}L_1\cdots L_p\beta\beta^{-[2(7-p)/(5-p)]}. \tag{D11}$$

Here, the action is evaluated in the Dp-frame (recall that the action is invariant under T-duality).

The value of the Euclidean action (above extremality) for the localized black $p-1$ brane solution is approximately (see below) given by[37]

$$S_{p-1}/N^2 = -C_{p-1}\lambda_p^{(p-4)/(6-p)}L_2\cdots L_p\beta\beta^{-[2(8-p)/(6-p)]}. \tag{D12}$$

For small enough L_1 (large enough L_1'), this is smaller than (D11). The transition between the uniform and localized $p-1$ branes happens when (D11) equals (D12):

$$\frac{\beta}{L_1} = \left(\frac{C_p}{C_{p-1}}\right)^{(5-p)(6-p)/4}\sqrt{\lambda_{p+1}L_1^{3-p}}. \tag{D13}$$

[36] If the fermion satisfies an antiperiodic (AP) boundary condition along the L_i cycle, the theory is mapped to a type 0 theory through the T-duality. Then, the bulk theory involves a tachyon and how the holographic description of gauge theory works in this frame is unclear. We thank Shiraz Minwalla for pointing this out.

[37] Improvements to this approximation are discussed in [71].

Here, we have used $\lambda_p = \lambda_{p+1}/L_1$. In (D12), one has used the approximation that the horizon size is much smaller than $1/L_p$. Since this is strictly not true near the phase transition point (where the horizon size is of the order of $1/L_1$), the estimate (D13) is approximate. See [5] for some details of this approximation.

Note that there are several arguments that this transition would be first order [5,23,51].

b. GL-type transition in the soliton sector

For bosonic theories in Euclidean spacetimes, the $\beta \leftrightarrow L_p$ interchange is a symmetry, provided all other radii are left unchanged. This is a symmetry of fermionic theories as well, provided the spin structures along t and x^p respect this symmetry. Thus, if there is a GL transition given by (D13), there must be a GL-type transition between a uniformly distributed solitonic $(p-1)$ brane to a localized solitonic $(p-1)$ brane when $1/L_1$ becomes too large. The transition is given by (D13) with a $\beta \leftrightarrow L_p$ interchange:

$$\frac{L_p}{L_1} = \left(\frac{C_p}{C_{p-1}}\right)^{(5-p)(6-p)/4} \sqrt{\lambda_{p+1} L_1^{3-p}}. \tag{D14}$$

c. The Scherk-Schwarz (SS) transition

This is a transition between the black p brane configuration (D1) and its solitonic counterpart (D6). If we use the same large U regulator for both the solutions, then (D5) and (D7) can easily be compared. The regulator term is the same in both the actions and can be ignored while comparing the two. Equating the two Euclidean actions, we get the transition temperature

$$\beta = L_p. \tag{D15}$$

Similarly, we can consider another solitonic solution by replacing $L_p \leftrightarrow L_k$, if L_k is also an AP circle. Then, further transitions will happen at $\beta = L_k$ and $L_p = L_k$.

Note that this transition is also expected to be first order [26].

3. D2 branes for various spin structures: generalities

In this section, we apply the general properties of the Dp solutions studied in the previous sections to the D2 brane on the 3-torus: $(t, x_1, x_2) = (t+\beta, x_1 + L_1, x_2 + L_2)$[38] and make a prediction for the phase structure of the two-dimensional gauge theory (3). As mentioned in Sec. V, we fix AP boundary condition for fermions along the x_2 circle. Then, there are four choices of boundary conditions for the fermions along the t and x_1 directions: (AP,AP), (AP,P), (P,AP), (P,P), where P denotes the periodic boundary condition and AP denotes the antiperiodic one. We will evaluate the phase structure of the gravitational system with these four boundary conditions. (Since the result in the (P,AP) case can be obtained from (AP,P) by exchanging $\beta \leftrightarrow L_1$, we will show the results in the (AP,P) case only.)

The order parameters of this theory are the Wilson loop operators winding around each cycle:

$$\begin{aligned}
\mathrm{Tr}U &= \frac{1}{N}\mathrm{Tr}P\exp\left(i\int_0^{\beta} A_0 dt\right),\\
\mathrm{Tr}V &= \frac{1}{N}\mathrm{Tr}P\exp\left(i\int_0^{L_1} A_1 dx_1\right),\\
\mathrm{Tr}W &= \frac{1}{N}\mathrm{Tr}P\exp\left(i\int_0^{L_2} A_2 dx_2\right).
\end{aligned} \tag{D16}$$

If the gravity solution has a contractible cycle (i.e. it wraps around a "cigar"), the expectation value of the corresponding Wilson loop operator is nonzero. If the solution is localized on a cycle, then also the expectation value of the corresponding Wilson loop operator is nonzero. However, if the solution wraps around a noncontractible cycle, the expectation value of the corresponding Wilson loop operator vanishes [23].

In order to derive the phase structure corresponding to Fig. 4, we will evaluate the phase structure of supergravity for each boundary condition by changing β and L_1 with a fixed L_2, which is related to a cutoff scale of the two-dimensional gauge theory (3) (see footnote 20).

From now on, we use units such that $\lambda_3 = 1$.

a. D2 on (AP,AP,AP) torus

We consider the phase structure of $D2$ branes on a 3-torus with (AP,AP,AP) boundary conditions. In this case, three solutions appear: $D2_{\beta(L_1,L_2)}$, $D2_{L_1(\beta,L_2)}$ and $D2_{L_2(\beta,L_1)}$. (Recall the notation at the end of Sec. D 1 a.) In this case, the theory does not have the P circle and only the SS transition (D15) happens. The phase structure is shown in Fig. 7.

As we have argued in Appendix D 1 b, we need to check the validity of the gravity solutions. Let us consider the solitonic solution $D2_{L_2(\beta,L_1)}$. From (D8), $L_2 \gg 1$ is required (in units where $\lambda_3 = 1$) to suppress the stringy excitations around the tip of the cigar. We need to check the condition related to the winding modes also. In order to suppress the winding modes, $L_1^{3/2}, \beta^{3/2} \gg L_2$ are required from (D9). The phase boundary AB and BC are given by $L_1 = L_2$ and $\beta = L_2$, and these conditions are satisfied on these boundaries in the large L_2 case. Thus, the $D2_{L_2(\beta,L_1)}$ phase is always reliable, if L_2 is large.

Next, we consider the black brane solution $D2_{\beta(L_1,L_2)}$. From (D8), $\beta \gg 1$ is required. Thus, this solution is not reliable when $\beta \sim O(1)$. We can see that the condition (D9) for the winding modes is satisfied in the region surrounded by the phase boundaries and $\beta \gg 1$.

[38] The notation L_1 in this section represents what is called L in the main text.

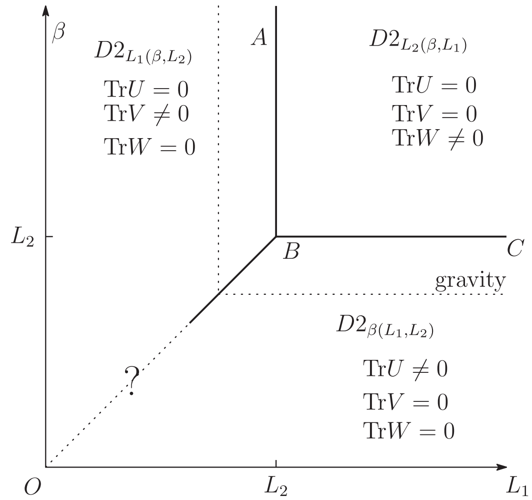

FIG. 7. Phase structure of the D2 brane on T^3 with (AP,AP,AP) boundary condition for large L_2. The gravity analysis is valid above the dotted line.

Therefore, the $D2_{\beta(L_1,L_2)}$ solution is reliable in the region indicated in Fig. 7. Similarly, the solitonic solution $D2_{L_1(\beta,L_2)}$ is reliable in the region indicated in Fig. 7.

Summing up these tests for the validity of the gravity analysis, the phase structure is reliable if L_2 is large and β and L_1 are above the dotted line in Fig. 7. This is, of course, a problem, since we are interested in the results in the $L_2 \to 0$ limit as we mentioned in Sec. V. We will discuss this problem in Appendix D 4.

b. D2 on (AP,P,AP) torus

In this case, four solutions appear: $D2_{\beta(L_1,L_2)}$, $D2_{L_2(\beta,L_1)}$, $D1_{L_2(\beta)}$ and $D1_{\beta(L_2)}$. The phase structure for large L_2 is shown in Fig. 8. The phase boundaries are given as

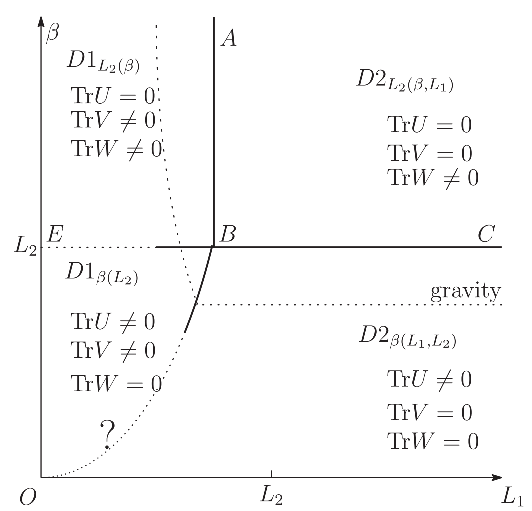

FIG. 8. Phase structure of the D2 brane on T^3 with (AP,P,AP) boundary condition for large L_2. The gravity analysis is reliable only in the region above the dotted line.

$$AB\colon L_1 = \left(\frac{C_1}{C_2}\right)^2 L_2^{2/3}, \qquad EC\colon \beta = L_2,$$
$$BO\colon \beta = \left(\frac{C_2}{C_1}\right)^3 L_1^{3/2}. \tag{D17}$$

Note that AB is the GL-type transition (D14), BO is the GL transition (D13) and EC is the SS transition (D15).

Through similar tests for the validity of gravity as before, we find that the gravity analysis is valid only in the region above the dotted line in Fig. 8. (Again, the gravity analysis in a small L_2 is invalid.)

c. D2 on (P,P,AP) torus

In this case, four solutions appear: $D2_{L_2(\beta,L_1)}$, $D1_{L_2(\beta)}$, $D1_{L_2(L_1)}$ and $D0_{L_2}$. The phase structure for a large L_2 is shown in Fig. 5. The phase boundaries are given by

$$AB\colon L_1 = \left(\frac{C_1}{C_2}\right)^2 L_2^{2/3}, \qquad BD\colon \beta = L_1,$$
$$DO\colon \beta = \left(\frac{C_0}{C_1}\right)^{5/2} L_2^{1/2} L_1^{1/4}. \tag{D18}$$

These are GL-type transitions (D15). Other lines can be obtained by $\beta \leftrightarrow L_1$. The gravity analysis is valid only in the region above the dotted line in Fig. 5 for large L_2.

We will adopt the phase structure in this boundary conclusion as a prediction for the gauge theory. The reason will be explained in the next section.

4. Conjectured phase diagram of 2D bosonic gauge theory

In the preceding subsections, we have obtained various phase structures from gravity for different spin structures (i.e., for different fermion boundary conditions). Since these results are valid only for large L_2, we need to extrapolate them to small L_2, where the bosonic gauge theory should appear (see footnotes 20 and 22).

From the viewpoint of the two-dimensional bosonic gauge theory, a holographic correspondence with the various gravity phase diagrams described in this section is problematic since the latter have a dependence on fermionic boundary conditions, while no such dependence obviously exists for the two-dimensional gauge theory (such dependences, however, exist for the three-dimensional SYM theory, which is more directly related to the gravity description). Indeed one such problem was pointed out in [67]. This argument is further developed in [68]. The arguments presented in these papers indicate that the phase transition in the bosonic gauge theory cannot be regarded as a continuation of the SS transition of gravity. Thus, in order to have a smooth continuation of phase boundaries between the holographic description and the two-dimensional gauge theory, we should avoid choosing the (AP,AP,AP) and (AP,P,AP) boundary conditions, in which the SS transition appear. For this reason, we choose the

(P,P,AP) case to read off the predicted phase structure from gravity.

Note that all the transitions in the (P,P,AP) case are of the GL-type, and are supposed to be first order phase transitions [5,23,51]. In this case, in addition to the uniformly distributed solitonic $(p-1)$ brane and localized solitonic $(p-1)$ brane discussed in D 2 b, nonuniformly distributed solitonic $(p-1)$ brane, which is always unstable, appears. These three solutions would correspond to the uniform, nonuniform and gapped distribution in the gauge theory (see Fig. 2). Indeed, the free energies of these gravity solutions are expected to satisfy a similar relation to those in the gauge theory shown in Fig. 3 through numerical study in general relativity [53]. This fact also supports our prediction from the gravity analysis.

[1] D. J. Gross, R. D. Pisarski, and L. G. Yaffe, Rev. Mod. Phys. **53**, 43 (1981).
[2] R. Narayanan and H. Neuberger, Phys. Rev. Lett. **91**, 081601 (2003).
[3] O. Aharony, *et al.*, and , J. High Energy Phys. 01 (2006) 140.
[4] R. Narayanan and H. Neuberger, Proc. Sci., LAT2007 (2007) 020 .
[5] M. Hanada and T. Nishioka, J. High Energy Phys. 09 (2007) 012.
[6] G. Mandal, M. Mahato, and T. Morita, J. High Energy Phys. 02 (2010) 034.
[7] M. Luscher, Nucl. Phys. **B219**, 233 (1983).
[8] G. 't Hooft, Nucl. Phys. **B153**, 141 (1979).
[9] T. Eguchi and H. Kawai, Phys. Rev. Lett. **48**, 1063 (1982).
[10] A. Gocksch and F. Neri, Phys. Rev. Lett. **50**, 1099 (1983).
[11] M. Unsal and L. G. Yaffe, J. High Energy Phys. 08 (2010) 030.
[12] R. Dijkgraaf, E. P. Verlinde, and H. L. Verlinde, Nucl. Phys. **B500**, 43 (1997).
[13] D. J. Gross and A. Neveu, Phys. Rev. D **10**, 3235 (1974).
[14] G. W. Semenoff, O. Tirkkonen, and K. Zarembo, Phys. Rev. Lett. **77**, 2174 (1996).
[15] N. Arkani-Hamed, S. Dimopoulos, and G. R. Dvali, Phys. Lett. B **429**, 263 (1998).
[16] N. Arkani-Hamed, S. Dimopoulos, and G. R. Dvali, Phys. Rev. D **59**, 086004 (1999).
[17] L. Randall and R. Sundrum, Phys. Rev. Lett. **83**, 3370 (1999).
[18] L. Randall and R. Sundrum, Phys. Rev. Lett. **83**, 4690 (1999).
[19] B. Sundborg, Nucl. Phys. **B573**, 349 (2000).
[20] O. Aharony, *et al.*, Adv. Theor. Math. Phys. **8**, 603 (2004).
[21] S. W. Hawking and D. N. Page, Commun. Math. Phys. **87**, 577 (1983).
[22] E. Witten, Adv. Theor. Math. Phys. **2**, 505 (1998).
[23] O. Aharony, J. Marsano, S. Minwalla, and T. Wiseman, Classical Quantum Gravity **21**, 5169 (2004).
[24] N. Itzhaki, *et al.*, Phys. Rev. D **58**, 046004 (1998).
[25] E. J. Martinec and V. Sahakian, Phys. Rev. D **59**, 124005 (1999).
[26] O. Aharony, *et al.*, Phys. Rep. **323**, 183 (2000).
[27] P. Basu, *et al.*, (work in progress).
[28] J. Polchinski, Phys. Rev. Lett. **68**, 1267 (1992).
[29] S. Dalley and I. R. Klebanov, Phys. Rev. D **47**, 2517 (1993).
[30] D. Kutasov, Nucl. Phys. **B414**, 33 (1994).
[31] G. Bhanot, K. Demeterfi, and I. R. Klebanov, Phys. Rev. D **48**, 4980 (1993).
[32] K. Demeterfi, I. R. Klebanov, and G. Bhanot, Nucl. Phys. **B418**, 15 (1994).
[33] A. Dhar, *et al.*, Int. J. Mod. Phys. A **10**, 2189 (1995).
[34] T. Hotta, J. Nishimura, and A. Tsuchiya, Nucl. Phys. **B545**, 543 (1999).
[35] C. R. Gattringer, L. D. Paniak, and G. W. Semenoff, Ann. Phys. (N.Y.) **256**, 74 (1997).
[36] P. Basu, B. Ezhuthachan, and S. R. Wadia, J. High Energy Phys. 01 (2007) 003.
[37] T. Morita, J. High Energy Phys. 08 (2010) 015.
[38] S. R. Wadia, Phys. Lett. B **93**, 403 (1980).
[39] A. M. Sengupta and S. R. Wadia, Int. J. Mod. Phys. A **6**, 1961 (1991).
[40] D. J. Gross and I. R. Klebanov, Nucl. Phys. **B352**, 671 (1991).
[41] J. Polchinski, Nucl. Phys. **B362**, 125 (1991).
[42] S. R. Das and A. Jevicki, Mod. Phys. Lett. A **5**, 1639 (1990).
[43] A. Jevicki and B. Sakita, Nucl. Phys. **B165**, 511 (1980).
[44] A. Dhar, G. Mandal, and S. R. Wadia, Mod. Phys. Lett. A **7**, 3129 (1992).
[45] D. J. Gross and E. Witten, Phys. Rev. D **21**, 446 (1980).
[46] N. Kawahara, J. Nishimura, and S. Takeuchi, J. High Energy Phys. 10 (2007) 097.
[47] T. Azuma, P. Basu, and S. R. Wadia, Phys. Lett. B **659**, 676 (2008).
[48] T. Azeyanagi, *et al.*, J. High Energy Phys. 03 (2009) 121.
[49] R. Gregory and R. Laflamme, Nucl. Phys. **B428**, 399 (1994).
[50] B. Kol, Phys. Rep. **422**, 119 (2006).
[51] T. Harmark, V. Niarchos, and N. A. Obers, Classical Quantum Gravity **24**, R1 (2007).
[52] E. Poppitz and M. Unsal, Phys. Rev. D **82**, 066002 (2010).
[53] H. Kudoh and T. Wiseman, Phys. Rev. Lett. **94**, 161102 (2005).
[54] J. Kiskis, R. Narayanan, and H. Neuberger, Phys. Lett. B **574**, 65 (2003).
[55] R. Narayanan, H. Neuberger, and F. Reynoso, Phys. Lett. B **651**, 246 (2007).
[56] J. Kiskis, Phys. Rev. D **74**, 054502 (2006).
[57] B. Lucini, M. Teper, and U. Wenger, J. High Energy Phys. 01 (2004) 061.
[58] M. Panero, Phys. Rev. Lett. **103**, 232001 (2009).

[59] S. Datta and S. Gupta, Phys. Rev. D **82**, 114505 (2010).
[60] M. Koren, Acta Phys. Pol. **2**, 489 (2009).
[61] S. Catterall, A. Joseph, and T. Wiseman, J. High Energy Phys. 12 (2010) 022.
[62] M. Hanada and I. Kanamori, Phys. Rev. D **80**, 065014 (2009).
[63] T. Azeyanagi, *et al.*, Phys. Rev. D **82**, 125013 (2010).
[64] O. Aharony, *et al.*, Phys. Rev. D **71**, 125018 (2005).
[65] K. Papadodimas, H. H. Shieh, and M. Van Raamsdonk, J. High Energy Phys. 04 (2007) 069.
[66] J. Liddle and M. Teper, Proc. Sci., LAT2005 (2006) 188.
[67] O. Aharony, J. Sonnenschein, and S. Yankielowicz, Ann. Phys. (N.Y.) **322**, 1420 (2007).
[68] G. Mandal and T. Morita, arXiv:1107.4048.
[69] Y. Hosotani, Ann. Phys. (N.Y.) **190**, 233 (1989).
[70] G. T. Horowitz and R. C. Myers, Phys. Rev. D **59**, 026005 (1998).
[71] T. Harmark and N. A. Obers, J. High Energy Phys. 09 (2004) 022.
[72] T. Harmark, V. Niarchos, and N. A. Obers, J. High Energy Phys. 10 (2005) 045.